Inorganic Chemistry

ARTICLE

pubs.acs.org/IC

# Unsymmetrical 1$\lambda^3$-1,2,4,6-Thiatriazinyls with Aryl and Trifluoromethyl Substituents: Synthesis, Crystal Structures, EPR Spectroscopy, and Voltammetry

René T. Boeré,* Tracey L. Roemmele, and Xin Yu

Department of Chemistry and Biochemistry, University of Lethbridge, Lethbridge, AB Canada T1K 3M4

Supporting Information

**ABSTRACT:** A general synthetic route to 3-trifluoromethyl-5-aryl-1$\lambda^3$-1,2,4,6-thiatriazinyl radicals was developed. X-ray structures were obtained for all five neutral radicals and show that they exist in the solid state as cofacial dimers linked by S···S contacts. X-ray structures were also obtained for two of the precursor chlorothiatriazines along with several aryl N-imidoylamidines, *p*-methoxybenzamidine, and N-chlorosulfonyl-N,N′-benzamidine. Cyclic voltammetric studies were performed on the $[R_2C_2N_3S]^{\bullet}$ radicals in $CH_3CN$ and $CH_2Cl_2$ with $[^nBu_4N][PF_6]$ as the supporting electrolyte under vacuum conditions in an all-glass electrochemical cell. The results provide quasi-reversible formal potentials for the $[R_2C_2N_3S]^{-/0}$ process in the range of −0.61 to −0.47 V, irreversible peak potentials for the $[R_2C_2N_3S]^{0/+}$ process from 0.59 to 0.91 V at lower concentrations, and the appearance of a second, reversible oxidation process from 0.69 to 0.94 V at higher concentrations (versus the $Fc^{0/+}$ couple; Fc = ferrocene). This behavior was indicative of monomer−dimer equilibrium in solution, as ascertained from digital models of the voltammograms. There is a small but measurable trend in both the oxidation and reduction potentials with varying remote aryl substituents. EPR spectra were obtained for all five neutral radicals in $CH_2Cl_2$ solutions, which confirm the concentration of the unpaired electron density on the heterocyclic core. Trends were also seen in the hyperfine splitting constants $a_N$ with varying remote aryl substituents. Calculations were performed for all three oxidation states of the $[R_2C_2N_3S]^{-/\bullet/+}$ monomeric rings; the resulting theoretical redox energies correlate well with solution phase voltammetric data.

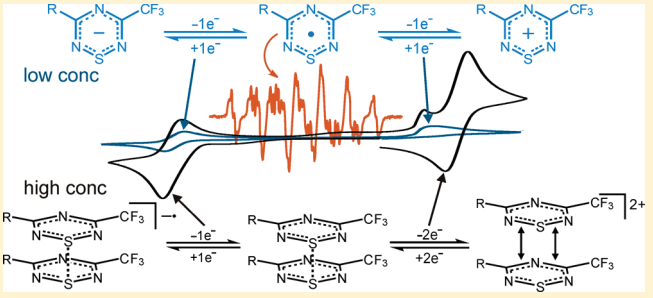


## INTRODUCTION

There is strong continuing interest in the synthesis and structural chemistry of sulfur−nitrogen−carbon heterocyclic free radicals, with an emphasis on applications to the design of molecular conductors and molecular magnetism.[1] This interest extends to transition-metal coordination complexes that incorporate such radicals as ligands—including spin-active ligands.[2] We have contributed to the electrochemical characterization of the redox properties of this whole class of compounds and, in particular, have characterized by solution electrochemistry the influence of aryl ring substituents on 5-aryl-1,2,3,4-dithiadiazolyls.[3]

In order to extend our approach to a new class of C,N,S radicals, we have developed a general synthetic route to the asymmetrically substituted 3-trifluoromethyl-5-aryl-1$\lambda^3$-1,2,4,6-thiatriazinyls (Chart 1). We recently communicated the utility of such thiatriazinyl radicals as novel $\pi$-donor ligands to the organometallic moiety $CpCr(CO)_2$;[4] here, we elaborate the chemistry of these heterocyclic free radicals, including structural characterization of novel intermediates and several final products in the solid state by X-ray crystallography, solution EPR spectroscopy, and a detailed electrochemical investigation interpreted in light of DFT calculations.

## RESULTS AND DISCUSSION

A primary goal of this work was the development of a more general route to 1,2,4,6-thiatriazinyl radicals which would allow for modification of the exocyclic substituents (Scheme 1). Various methods have been attempted to prepare both symmetric and asymmetrically substituted thiatriazines.[5] Amidines have been reported to react with $S_3N_3Cl_3$ to form 1-chloro-1,2,4,6-thiatriazines.[5e,f] In this work, we first converted amidines into N-imidoylamidines and found that these, when passivated as hydrochlorides, afford 1-chloro-1,2,4,6-thiatriazines by direct reaction with sulfur dichloride in high yield.[5b,6] An established literature procedure was used to prepare the *para*-substituted benzamidine hydrochlorides,[7] but the free bases **1a**−**e** have not previously been reported. Full characterization of these useful intermediates is provided in the Experimental Section, and the crystal structure of **1a** is presented in Figure S1 (Supporting Information).

**Aryl N-Imidoylamidines.** In contrast to amidine chemistry, aryl N-imidoylamidines have received less attention, although

**Received:** February 25, 2011
**Published:** May 03, 2011

**Chart 1. The 3-Trifluoromethyl-5-aryl-1$\lambda^3$-1,2,4,6-thiatriazinyls**

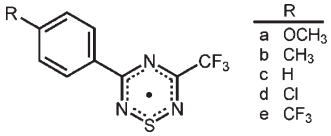


**Scheme 1. Synthetic Route to the 3-Trifluoromethyl-5-aryl-1,2,4,6-thiatriazines**

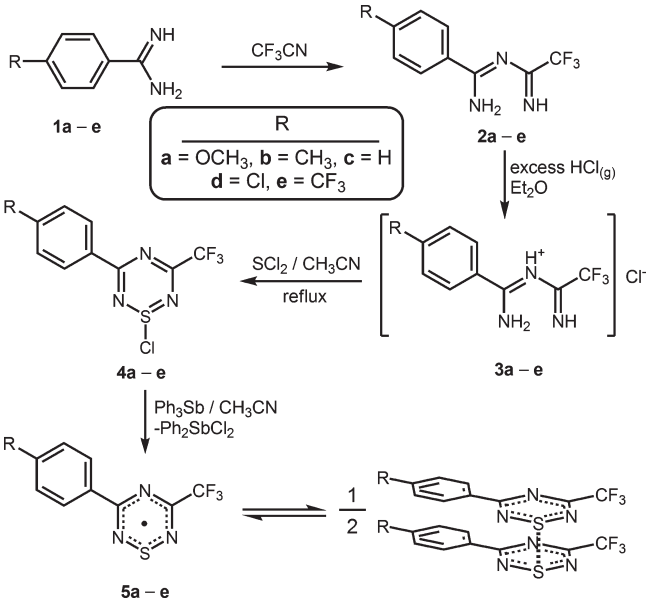


several preparative routes have been reported.[8] In this work, it was found that direct reaction of trifluoroacetonitrile with the free-base amidines gave the desired imidoylamidines in high yields in accordance with the report by Schaeffer.[9] The colorless sublimed products were found to be pure by $^1$H and $^{13}$C NMR spectroscopy, MS, and elemental analysis. The expected signals for hydrogen atoms attached to carbon were observed in $^1$H NMR spectra recorded in $CDCl_3$ (Table S1, Supporting Information). Three separate NH peaks are also observed (Figure S2, Supporting Information), indicating nonequivalency of the hydrogen atom environments. The signals resonating around 11 and 6.7 ppm are noticeably broadened compared to the one near 9 ppm, indicating a higher rate of exchange between the former.

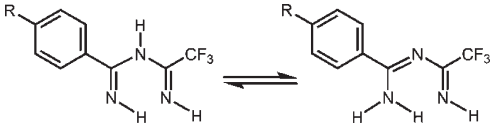

These results are consistent with either of the above tautomers, i.e., either with hydrogen attached to three different N atoms as on the left or, as on the right, with one imino and two amino hydrogen atoms in which the latter are nonequivalent due to strong intramolecular hydrogen bonding. The solid-state structure (Figure 1) shows the dominance of the imino−amino tautomer but also shows H-bonding of H1B to the backbone

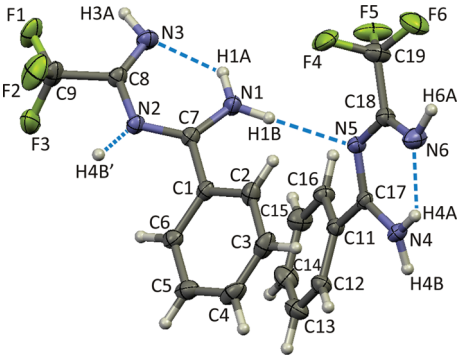


**Figure 1.** Thermal ellipsoid (30%) plot showing the two independent hydrogen-bonded molecules of **2c** as found in the crystal at −100(2) °C along with an additional H4B′ atom to indicate how the chain propagates in the lattice. The H1B−N5 and H4B′−N2 bonds can be viewed as incipient tautomerism leading to the diimine isomer. Only the principal components of the disordered $CF_3$ groups are shown for clarity (Figures S3 and S4, Supporting Information, are plots of **2a** and **2e**.).

nitrogen atom N5, which, if exchange occurred, would interconvert it to the diimine. In the $^{13}$C NMR spectra, seven distinct carbon peaks (Table S2) were observed, which are attributable to the seven different types of carbon atoms in **2a**−**e**.

X-ray structures of imidoylamidines are rare. In fact, no structures of unsubstituted imidoylamidines have been reported in the Cambridge Crystal Structure Database (CSD, version 5.31, updated Nov. 2009), and only one structure of an imidoylamidinium salt is known (with $[Se_2Cl_{10}]^{2-}$ as the counterion).[10] However, crystal structures of imidoylamidinate anions coordinated to various metals are known,[11] and the structure of the related parent biguanide has been reported.[12] Colorless crystalline plates of **2a**, **2c**, and **2e** were grown by sublimation in a three-zone tube furnace under a dynamic vacuum, and their structures were determined at low temperatures by X-ray diffraction. All three crystal structures contain two crystallographically independent molecules which display very similar inter- and intramolecular hydrogen bonding,[13] as shown by dashed lines in Figure 1 for compound **2c** as a representative example. The atom numbering scheme is the same for all three structures to facilitate comparison; the H-bonding data for **2a**, **2c**, and **2e** are discussed in the Supporting Information (Table S3).

The average bond lengths and angles determined from all six crystallographically independent molecules of **2a**, **2c**, and **2e** are shown in Figure 2. This clearly shows that C8−N3 is short, characteristic of an imine, while C7−N1 and C7−N2 are identical within esd and of intermediate length, characteristic of a highly delocalized amidine. Aryl/$CF_3$ substitution therefore leads to a rather unsymmetrical imidoyl amidine geometry, approximating an imino-substituted amidine.

**Conversion to N-Imidoylamidine Hydrochlorides.** Direct reaction between **2c** and sulfur dichloride to form **4c** resulted in low yields of the product as an intractable oil that proved hard to purify. However, pacifying the reactive nitrogen base with HCl increased the yield of **4c** significantly and afforded a low-melting solid. Therefore, all of the imidoylamidines were converted with HCl(g) in dry diethyl ether to the corresponding hydrochloride salts **3a**−**e**, which precipitated as white, insoluble solids that were characterized by infrared spectroscopy. Each adduct has a unique fingerprint region but similar broad bands in the 3300 cm$^{-1}$ range characteristic for NH stretches involved in hydrogen bonding.


dx.doi.org/10.1021/ic2003996 |*Inorg. Chem.* 2011, 50, 5123–5136

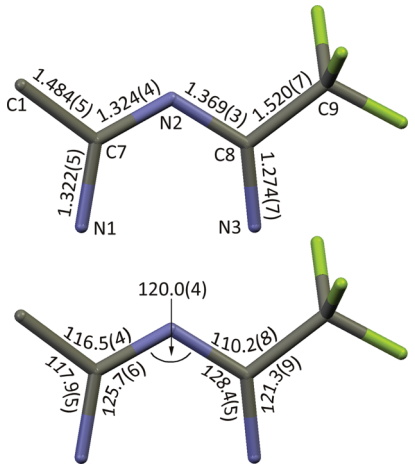


**Figure 2.** Average bond lengths (Å, top) and angles (deg, bottom) from crystal structures of the six independent imidoylamidine molecules found in **2a**, **2c**, and **2e**. Errors are standard deviations.

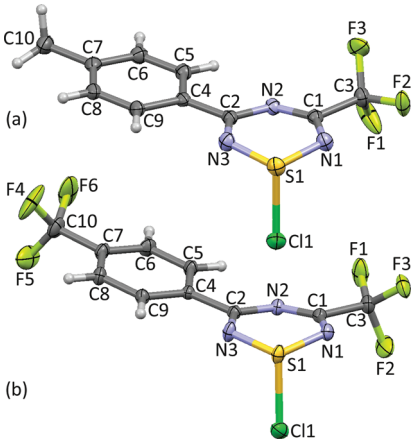


**Figure 3.** Thermal ellipsoid (30%) plots with atom numbering schemes showing the molecular structures of (a) **4b** and (b) **4e** as they are found within the crystal lattices at −100(2) °C. Only the principal components of the disordered $CF_3$ groups are shown.

**1-Chloro-3-trifluoromethyl-1,2,4,6-thiatriazines.** An excess of $SCl_2$ was used to ensure the completion of the reaction of the imidoylamidine hydrochloride salts **3a**−**e** to the 1-chloro-thiatriazines **4a**−**e**. Crude yields were typically high (>80%), and these materials were used without further purification in the synthesis of the radicals. $^1$H NMR spectra (Table S4, Supporting Information) confirmed ring formation through the absence of NH signals, and only the phenyl and *para*-substituted hydrogen atoms appear in the spectra between 7.0 and 8.6 ppm. The signals of $H_1$, *meta* to the thiatriazine core, are weakly affected by heterocycle formation, shifting only ∼0.10 ppm downfield compared to the imidoylamidines. However, the signals of $H_2$, *ortho* to the heterocyclic core, are shifted downfield by ∼0.60 ppm. This is diagnostic for the formation of a thiazyl ring; for example, the chemical shifts of the *ortho* hydrogen atoms in comparably substituted 1,5-dithia-2,4,6,8-tetrazocine heterocycles are very similar to those of **4a**−**e**.[14] $^{13}$C NMR was not obtained due to instability of the compounds to hydrolysis. However, extremely moisture-sensitive X-ray-quality crystals could be grown for **4b** and **4e** from acetonitrile solutions at −35 °C, and the crystal structures were determined at low temperatures. These structures confirm the formation of the six-membered ring with an almost perpendicular S−Cl bond, as shown in Figure 3. The $C_2N_3$ atoms are coplanar (maximum deviation 0.047(1) Å), with the sulfur atoms tipped slightly out of the plane (0.288(2) Å, **4b**; 0.323(2) Å, **4e**). The interatomic distances in **4b** and **4e** are quite comparable. Averaged bond lengths and angles from the two structures are presented in Figure 4. The phenyl rings in both structures have average C−C bond lengths of 1.389(10) Å and are essentially coplanar with the heterocyclic core. The packing of **4e** shows regular stacks aligned with the crystallographic *c* axis without any significant short contacts, but **4b** has typical S-($\delta^+$)−N($\delta^-$) short contacts between pairs of rings (Figure S5, Supporting Information).[1d]

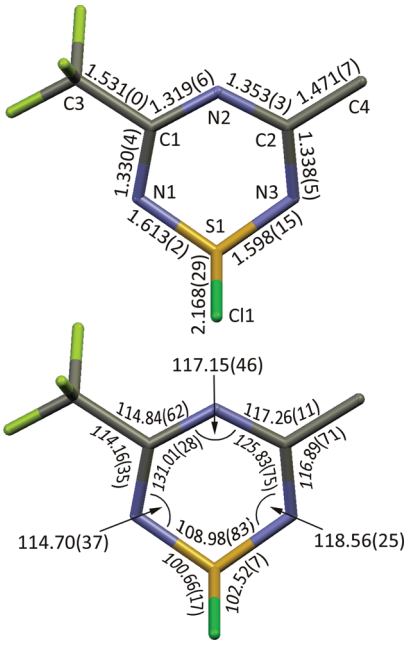


**Figure 4.** Average bond lengths (Å, top) and angles (deg, bottom) with standard deviations from crystal structures of the 1-chlorothiatriazines **4b** and **4e**.

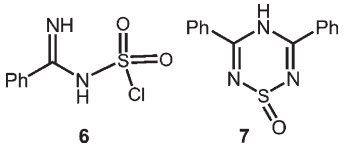


**6** **7**

The sensitivity of **4** to moisture is highlighted by the hydrolysis of **4c** from adventitious $H_2O$ in $CH_3CN$ to give **6** as colorless blocks suitable for X-ray analysis (Figures S6−S8, Supporting Information). The hydrolysis product **6** surprisingly retains the S−Cl bond (unlike {PhCN}$_2${NH}S=O, **7**),[15] but a $CF_3CH$=NH moiety is eliminated while the sulfur is converted to oxidation state VI.

**5-Aryl-3-trifluoromethyl-1,2,4,6-thiatriazinyls.** Several reducing agents have been used previously to effect the reductive elimination of the chloride ion from 1-chloro-1,2,4,6-thiatriazines. In early work, sodium verdazyl was often used.[5] Here, we employed triphenylantimony because of its general utility in the


dx.doi.org/10.1021/ic2003996 |*Inorg. Chem.* 2011, 50, 5123–5136

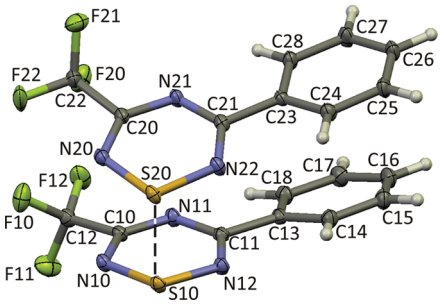


**Figure 5.** Thermal ellipsoid (30%) plot and atom numbering scheme showing the solid-state face-to-face and head-to-head dimerization of **5c**, which comprises the asymmetric unit in the lattice at −100(2) °C. The dashed line indicates the close contact between sulfur atoms, for which the S10···S20 distance is 2.625(1) Å. The structure of **5a** (Figure S9, Supporting Information) is very similar, with an S10···S20 distance of 2.6370(3) Å.

reduction of thiazyl halides.[5e,f] A half-molar ratio of solid triphenylantimony was added by a solids-addition bulb to acetonitrile solutions of **4a**−**e** after careful removal of oxygen via freeze−thaw−degassing. Reduction to the radical was immediate in all cases, as the solution turned from a clear dark red to a dark purple (almost black) solution with the precipitation of some solid. Precipitated crude products were purified by sublimation in a three zone tube furnace and produced X-ray-quality plates of the radicals **5a**−**e**. Diffraction data were obtained at −100 ± 2 °C and the structures solved and refined at this temperature. However, in the case of **5b**, persistent high R factors were encountered, and hence the structure was redetermined at RT with better results. Formation of a superlattice is suspected at the lower temperature. In each case, the solid-state structures display the same face-to-face and head-to-head (presumably diamagnetic) dimers obtained previously for bis(3,5-diphenyl-1,2,4,6-thiatriazinyl) (**8**),[5e] despite the presence of the bulky $CF_3$ groups. For both **5a** and **5c**, one kind of crystallographically independent dimer is observed in their crystal lattices (Figure 5). For **5b** and **5d**, two sets of wedge-shaped dimers are found stacked back-to-front in the lattice (Figure 6).

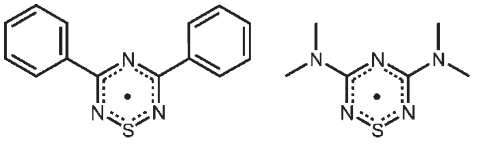


**8** **9**

The shortest contact between $C_2N_3S$ rings is always through the sulfur atoms, with an average distance of 2.643(21) Å. This is longer than a normal disulfide linkage but within range of other known thiatriazinyls such as **8**,[5e] whose shortest contact is 2.666(3) Å, and 3,5-bis(dimethylamino)-1,2,4,6-thiatriazinyl (**9**), whose shortest contact is again through the sulfur atoms at 2.5412(8) Å.[16] Average bond lengths and angles were calculated for the entire series **5a**−**e**, and the results are presented in Figure 7. The average S−N bond length over both bonds (SX0−NX0 and SX0−NX2, X = 1−4) is 1.633(10) Å, which is shorter than the S−N single bond in $S_4N_4H_4$ (1.665 Å) and longer than the N- − -S bond in $S_4N_4$ (1.616 Å). The average C−N bond length in the ring is 1.332(16) Å, longer than an average C═N double bond (∼1.270(15) Å)[17] and shorter than

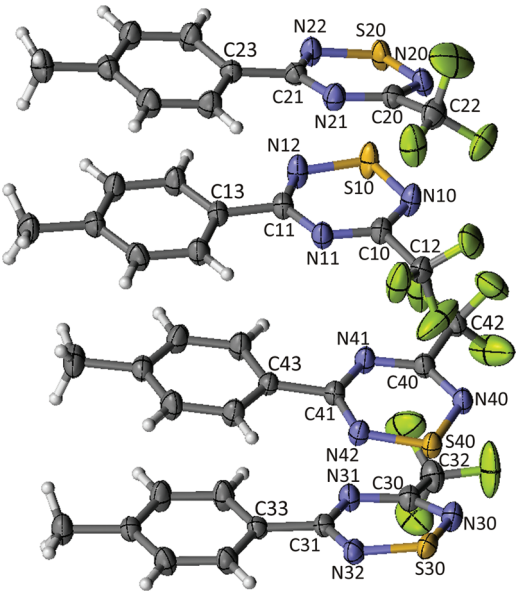


**Figure 6.** Thermal ellipsoid (30%) plot with atom numbering scheme showing the molecular structure of **5b** found within the crystal lattice at 23(2) °C. Four crystallographically independent molecules form two distinct dimers. The S10···S20 distance is 2.684(1) Å, and the S30···S40 distance is 2.6515(8) Å. A very similar arrangement is found in the lattice for **5d** (Figure S10, Supporting Information) with S10···S20 and S30···S40 distances of 2.659(1) Å and 2.635(1) Å, respectively.

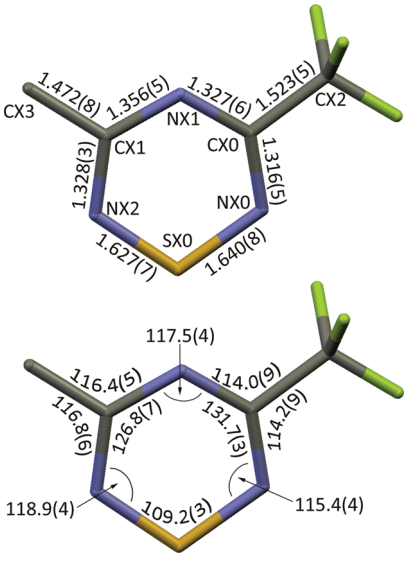


**Figure 7.** Average bond lengths (Å, top) and angles (deg, bottom) with standard deviations in 1,2,4,6-thiatriazinyls determined from five crystal structures. A common numbering scheme was used among crystallographically independent monomers (X = 1−4). The average intradimer short S···S contact distance is 2.643(21) Å.

an average C−N single bond (1.472(5) Å). A typical heterocyclic C- − -S bond length is approximately 1.352(5) Å.[17] The asymmetric substitution pattern seen in **5a**−**e** allows for a comparison of the bond lengths and angles with the symmetric diphenyl and dimethylamino analogues **8** and **9**. The C−N bond lengths are very similar, as are the S−N bond lengths with only the S−N bond closest to the $CF_3$ group averaging slightly longer than in **8**.


dx.doi.org/10.1021/ic2003996 |*Inorg. Chem.* 2011, 50, 5123–5136

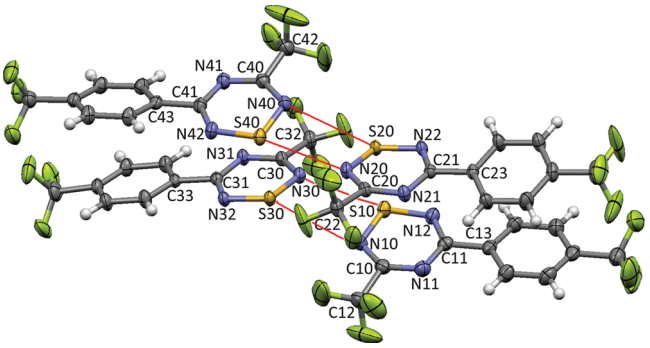


**Figure 8.** Thermal ellipsoid (30%) plot with atom numbering scheme showing the molecular structure of **5e** found within the crystal lattice at −100(2) °C. Four crystallographically independent molecules form into two distinct dimers with intradimer S10···S20 and S30···S40 distances of 2.6237(9) Å and 2.6255(8) Å, respectively. These dimers associate into a single tetrameric set through $S(\delta^+)-N(\delta^-)$ interactions (shown in red). The S20···N30 and S30···N20 distances are 3.169(2) Å and 3.199(2) Å, while the S40···N20 and S10···N30 distances are 3.082(2) Å and 3.034(2) Å, respectively. The two dimers are out of register with each other.

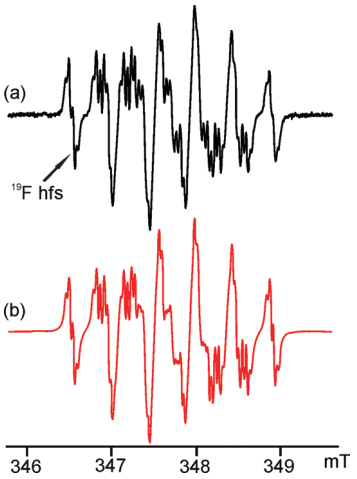


**Figure 9.** (a) Experimental and (b) simulated EPR spectra of **5d** in $CH_2Cl_2$ at 18 °C, modulation amplitude 0.01 mT, modulation frequency 100 kHz. Simulations were performed with WinSim (version 0.98, 2002)[19] software using a 100% Lorentzian line shape.

The bond angles within the heterocyclic core are significantly less symmetrical with asymmetric substitution on the ring. Thus, the internal angles at the carbon of attachment of the $CF_3$ group are noticeably larger than in **8**.[5e] Correspondingly, the average internal angles at sulfur are noticeably smaller than those in **8**.

In all five structures, the many independent $C_2N_3S$ rings are almost planar (deviations in the range of 0.003−0.054 Å). The mean planes of each set of dimers are tipped toward each other such that the shortest contacts are always S···S, and the planes intersect with angles between normals in the range of 5−17°. Three distinct packing modes are found in the solid state among these five thiatriazinyl structures. In **5a** and **5c**, there is a simple 2 + 2 mode, wherein two dimeric units (Figure 5) are centrosymmetrically associated through sideways $S(\delta^+)\cdots N(\delta^-)$ short contacts. However, the pairs of dimers are essentially coplanar in the case of **5a** (Figure S11, Supporting Information), while in **5c** they are almost exactly out of register (Figure S12, Supporting Information). These tetrameric units are isolated from other such units in the crystal lattice. Sideways S···N contacts range from 2.941(1) to 3.341(1) Å. In **5b** and **5d**, there are four independent molecules that form two sets of typical dimers. However, the two sets of dimers are each associated with each other through $S(\delta^+)\cdots N(\delta^-)$ short contacts (Figures S13 and S14, Supporting Information). Interestingly, in each structure, one such tetrameric unit is closer to the coplanarity that is observed in **5a**, while a second is out of register as in **5c**. The variation in sideways S···N contacts observed in these two structures is larger, from 3.025(2) to 3.551(2) Å. The final example is **5e** (Figure 8), for which four independent thiatriazinyls form *one* tetramer in the asymmetric unit. The sideways $S(\delta^+)\cdots N(\delta^-)$ interactions for this structure range from 3.034(2) to 3.199(2) Å, and the association is out of register as in **5c**. This structure is particularly interesting because there is a further interaction between neighboring rings, leading to a partial overlap of two adjacent tetramers (Figures S15 and S16, Supporting Information). The shortest atomic contacts are S40···C41′ at 3.447(2) Å. This structure contains the most extensive set of interactions between thiatriazinyls ever reported, but, although eight radicals are thereby associated, the interactions do not extend throughout the lattice.

**EPR Spectroscopy.** The 1,2,4,6-thiatriazinyls are members of a larger class of unsaturated C,N,S compounds for which stable neutral free radicals can be generated.[1a] In this work, the trifluoromethyl thiatriazinyls **5a**−**e** were generated by dissolving high purity sublimed crystals in dichloromethane inside vacuum sealed EPR tubes. In all cases, well-defined EPR spectra with high signal-to-noise ratios were obtained, displaying complex splitting patterns due to coupling to the three nonequivalent nitrogen nuclei in the thiatriazinyl ring along with three equivalent fluorine atoms of the directly attached $CF_3$ groups, which cause each subpeak to split into small quartets. Excellent agreement was obtained between the experimental and simulated EPR spectra for all five compounds (Figure 9 shows a typical example; see also Figures S17−S20, Supporting Information). However, the assignment of the hyperfine splitting (hfs) to the three nitrogen atoms required input from quantum calculations. The electronic structures of **5a**−**e** were determined from UB3LYP/6-31G(d) hybrid-DFT calculations (using Gaussian 98)[18] for the monomeric radicals in the gas phase. Full geometry optimization was undertaken for each structure, and frequency calculations confirmed the geometries to be minima. The experimental and calculated hfs constants are compiled in Table 1.

The unpaired electron occupies a $\pi$-SOMO which is delocalized over the heterocyclic core, a representation of which is shown in Figure 10 using **5b** as a typical example. The largest coefficient is on sulfur, but there is considerable unpaired electron density on each of the three nitrogen atoms and to a lesser extent on the carbon atoms in the ring. There are small coefficients on the fluorine atoms of the directly bound $CF_3$ group, as well as on the phenyl carbon atoms. There is, however, no experimental evidence for hyperfine coupling to the aryl ring hydrogen atoms, and hfs from $^{19}$F is likely to result mostly from spin polarization.

In each case, there are three distinct $a_N$ values, except for **5a**, where two of the values are nearly identical. (Such accidental degeneracy of symmetry-nonequivalent nitrogen atoms has been reported for 3,5-bis(4-methoxyphenyl)-1,2,4,6-thiatriazinyl, for which all three nitrogen atoms appear to have identical hfs of 0.3927 mT.)[20] The trends in the hfs with the remote *para* R


dx.doi.org/10.1021/ic2003996 |*Inorg. Chem.* 2011, 50, 5123–5136

**Table 1. Experimental and Calculated[a] EPR Spectroscopic Data for 5a−e**

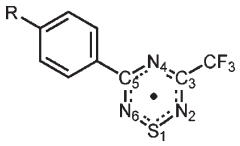


| | $a_{N2}$ | | $a_{N4}$ | | $a_{N6}$ | | $a_{C3,5(avg)}$ | | $a_{S1}$ | $a_{F(avg)}$ | |
|---|---|---|---|---|---|---|---|---|---|---|---|
| cmpd | expt (mT) | calc (mT) | expt (mT) | calc (mT) | expt (mT) | calc (mT) | expt (mT) | calc (mT) | calc[b] (mT) | expt[c] (mT) | calc (mT) |
| **5a** | 0.310 | 0.297 | 0.435 | 0.409 | 0.436 | 0.460 | 0.705 | −0.518 | 0.555 | 0.032 | −0.063 |
| **5b** | 0.320 | 0.309 | 0.444 | 0.418 | 0.429 | 0.443 | 0.545 | −0.531 | 0.555 | 0.036 | −0.068 |
| **5c** | 0.325 | 0.313 | 0.445 | 0.422 | 0.425 | 0.437 | 0.675 | −0.536 | 0.555 | 0.039 | −0.069 |
| **5d** | 0.324 | 0.313 | 0.446 | 0.422 | 0.419 | 0.433 | 0.572 | −0.534 | 0.558 | 0.040 | −0.068 |
| **5e** | 0.332 | 0.319 | 0.454 | 0.428 | 0.404 | 0.423 | 0.666 | −0.542 | 0.558 | 0.044 | −0.070 |

[a] From UB3LYP calculations, multiplied by a scaling factor of 0.81. [b] Sulfur hfs was not observable due to the very small natural abundance of this isotope. [c] hfs is to the three fluorine atoms in the directly bound $CF_3$ group.

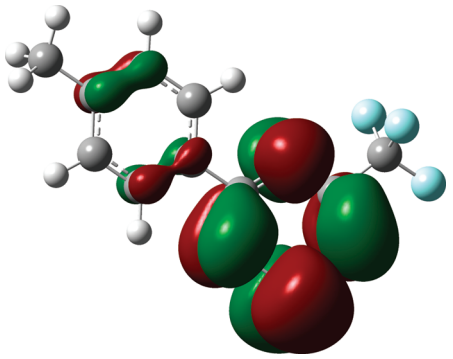

**Figure 10.** Kohn−Sham isosurface of the $\pi$-SOMO of **5b** from a UB3LYP/6-31G(d) calculation.

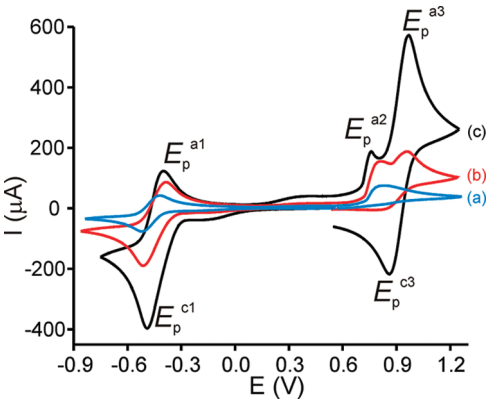


**Figure 11.** Overlapping CVs of the redox couples of **5e** in $CH_3CN$ solution (0.1 M [$^n$Bu$_4$N][PF$_6$]) at (a) dilute concentration (blue), (b) moderate concentration (red), and (c) high concentration (black).

substituents on the phenyl ring are quite convincing. As controls, we can cite the powerfully $\pi$-electron donating $NMe_2$ groups directly bound in 3,5-bis(dimethylamino)-1,2,4,6-thiatriazinyl (**9**),[20] in which $a_{N2} = a_{N6}$ is twice as large as $a_{N4}$. Conversely, with two powerfully electron withdrawing $CF_3$ and $CCl_3$ groups directly attached in 3,5-bis(trifluoromethyl)-1,2,4,6-thiatriazinyl[24] and 3,5-bis(trichloromethyl)-1,2,4,6-thiatriazinyl,[5d,20b] $a_{N4}$ is found to be larger by about 40% than $a_{N2}$ and $a_{N6}$. The hyperfine splitting constants of **5a**−**e** are intermediate between these extremes, as expected. Nevertheless, as the remote *para* substituents become more electron donating (from **e** to **a**), the $a_{N6}$ value increases due to greater spin density on the N═S═N region of the ring. The spin density on the remaining nitrogen atoms decreases correspondingly, such that the sums of $a_N$ values are found to be 1.190(5) for all five exemplars (standard deviation). Moreover, the variation in $a_N$ values smoothly follows Hammet $\sigma$(p) coefficients (Figure S21, Supporting Information). Thus, EPR spectroscopy proves to be a very sensitive probe of the unpaired spin density on thiatriazinyl rings. The directly bound $CF_3$ group causes further splitting of the EPR signals into quartets, implying rotational averaging of the three fluorine nuclei, but the $a_F$ values are small. Similar $a_F$ values have been reported for 3,5-bis(trifluoromethyl)-1,2,4,6-thiatriazinyl.[20]

**Voltammetry.** The study of redox active heterocycles requires handling of low concentrations of free radicals in solution which are highly susceptible to decomposition from oxygen or hydrolysis by adventitious moisture. An all-glass electrochemical cell sealed under vacuum conditions which has been described previously was used in this work to avoid interference.[21] Cyclic voltammetric studies were performed in both $CH_2Cl_2$ and $CH_3CN$ solutions at temperatures of 20 ± 2 °C and scan rates of $\nu$ = 0.1−10 V s$^{-1}$. The voltammetric results at full concentration are summarized in Table 2.

The 1,2,4,6-thiatriazinyls are very soluble in dichloromethane and moderately soluble in acetonitrile. In all cases, the electrochemical response changed with analyte concentration, with the appearance of a new redox couple at more positive potentials as the solution became more concentrated (Figure 11). This change correlated with the color of the solution (from pale yellow to deep brown) as more analyte was added. From the current response of the CV data, the active concentrations from voltammetry taken when the solutions were pale yellow are estimated to be 10−20 times lower than the nominal concentration values listed in Table 2. At very low concentrations (evidenced by a pale yellow color in solution), the peaks associated with a reduction of neutral material ($E_p^{c1/a1}$) have a large return wave over a range of scan rates, while that for oxidation ($E_p^{a2}$) shows no return wave at scan rates up to 10 V s$^{-1}$.


dx.doi.org/10.1021/ic2003996 |*Inorg. Chem.* 2011, 50, 5123–5136

**Table 2. Voltammetry Data for Compounds 5a−e in $CH_3CN$ and $CH_2Cl_2$ at Full Concentration[a]**

| cmpd | conc. (mM) | $E_p^{c1}$ (V) | $E_p^{a1}$ (V) | $E_m$ (V)[b] | $E_p^{a2}$ (V)[c] | $E_p^{c3}$ (V) | $E_p^{a3}$ (V) | $E_n$ (V)[d] | $E_{cell}$ (V)[e] |
|---|---|---|---|---|---|---|---|---|---|
| | | | | $CH_3CN$ solns with 0.1 M [$^n$Bu$_4$N][PF$_6$] supporting electrolyte | | | | | |
| **5a**[f] | 7.3 | −0.64 | −0.51 | −0.58 | 0.59 | 0.62 | 0.76 | 0.69 | 1.27 |
| **5b** | 6.3 | −0.60 | −0.51 | −0.56 | 0.67 | 0.71 | 0.81 | 0.76 | 1.32 |
| **5c**[g] | 10.0 | −0.60 | −0.48 | −0.54 | 0.73 | 0.74 | 0.89 | 0.82 | 1.36 |
| **5d**[h] | 11.0 | −0.55 | −0.45 | −0.50 | 0.74 | 0.78 | 0.90 | 0.84 | 1.34 |
| **5e**[i] | 6.7 | −0.51 | −0.42 | −0.47 | 0.84 | 0.85 | 0.96 | 0.91 | 1.38 |
| | | | | $CH_2Cl_2$ solns with 0.4 M [$^n$Bu$_4$N][PF$_6$] supporting electrolyte | | | | | |
| **5a**[j] | 10.0 | −0.66 | −0.55 | −0.61 | 0.66 | 0.66 | 0.78 | 0.72 | 1.33 |
| **5b** | 8.7 | −0.66 | −0.54 | −0.60 | 0.71 | 0.74 | 0.86 | 0.80 | 1.40 |
| **5c**[k] | 11.0 | −0.64 | −0.52 | −0.58 | 0.76 | 0.78 | 0.92 | 0.85 | 1.43 |
| **5d**[l] | 9.0 | −0.63 | −0.47 | −0.55 | 0.81 | 0.79 | 0.98 | 0.89 | 1.44 |
| **5e**[m] | 6.7 | −0.55 | −0.44 | −0.50 | 0.91 | 0.87 | 1.01 | 0.94 | 1.44 |

[a] Reported vs $Fc^{0/+}$ on a Pt working electrode, $\nu = 0.2$ V s$^{-1}$, $T = 20 \pm 2$ °C. [b] $E_m = [E_p^{a1} + E_p^{c1}]/2 \approx E^{0/}$. [c] Irreversible wave observed. [d] $E_n = [E_p^{a3} + E_p^{c3}]/2 \approx E^{0/}$. [e] $E_{cell} = E_n - E_m$. [f] IRR oxidation wave at 1.75 V. [g] IRR reduction wave at −1.87 V. [h] IRR reduction wave at −1.80 V. [i] IRR reduction wave at −2.07 V. [j] IRR oxidation wave at 1.84 V. [k] IRR reduction wave at −1.78 V. [l] IRR reduction wave at −1.76 V. [m] IRR reduction wave at −1.65 V.

**Table 3. Voltammetry Data for Compounds 5a−e in $CH_3CN$ and $CH_2Cl_2$ at Low Concentration[a]**

| cmpd | $E_p^{c1}$ (V) | $E_p^{a1}$ (V) | $E_m$ (V)[b] | $E_p^{a2}$ (V)[c] | $E_{cell}$ (V)[d] |
|---|---|---|---|---|---|
| | | $CH_3CN$ solns with 0.1 M [$^n$Bu$_4$N][PF$_6$] supporting electrolyte | | | |
| **5a** | −0.60 | −0.54 | −0.57 | 0.59 | 1.13 |
| **5b** | −0.59 | −0.52 | −0.56 | 0.67 | 1.19 |
| **5c** | −0.57 | −0.50 | −0.54 | 0.73 | 1.23 |
| **5d** | −0.53 | −0.46 | −0.50 | 0.74 | 1.20 |
| **5e** | −0.51 | −0.41 | −0.46 | 0.84 | 1.25 |
| | | $CH_2Cl_2$ solns with 0.4 M [$^n$Bu$_4$N][PF$_6$] supporting electrolyte | | | |
| **5a** | −0.54 | −0.47 | −0.51 | 0.66 | 1.13 |
| **5b** | −0.53 | −0.47 | −0.50 | 0.71 | 1.18 |
| **5c** | −0.50 | −0.45 | −0.48 | 0.76 | 1.21 |
| **5d** | −0.49 | −0.42 | −0.46 | 0.81 | 1.23 |
| **5e** | −0.45 | −0.38 | −0.42 | 0.91 | 1.29 |

[a] Reported vs $Fc^{0/+}$ on a Pt working electrode, $\nu = 0.2$ V s$^{-1}$, $T = 20 \pm 2$ °C. [b] $E_m = [E_p^{a1} + E_p^{c1}]/2 \approx E^{0/}$. [c] Irreversible wave observed. [d] $E_{cell} = E_p^{a2} - E_p^{a1}$.

As the concentration increased (evidenced by development of a brown color), a second oxidation process ($E_p^{a3/c3}$) appeared at a more positive potential, and in the limit, this process displayed return waves of comparable peak current height ($I_p^{c3}/I_p^{a3} = 0.95$ (**5a**), 0.96 (**5b**), 0.89 (**5c**), 0.93 (**5d**), 0.93 (**5e**)) under all of the conditions used in this study. Figure 11 shows overlapping traces at three different concentrations of **5e**. At the highest concentration, process $E_p^{a2}$ is just a residual shoulder on the reversible wave at more anodic potential. Much the same thing occurred for all five compounds in both solvents. In each case, there was only a single potential associated with reduction of neutral material at all concentrations studied.

When the solutions are at the full indicated concentration (Table 2), the potential range for the "reduction" process is from −0.58 to −0.47 V vs $Fc^{0/+}$ in $CH_3CN$ and −0.61 to −0.50 V vs $Fc^{0/+}$ in $CH_2Cl_2$ and has an overall change of 0.11 V in both solvents. The potential range for the "oxidation" process is from 0.69 to 0.91 V vs $Fc^{0/+}$ in $CH_3CN$ and 0.72 to 0.94 V vs $Fc^{0/+}$ in $CH_2Cl_2$ and has an overall change of 0.22 V. The average $E_{cell}$ values ($E_{cell} = E_n - E_m$) are 1.33 ± 0.04 V in $CH_3CN$ and 1.41 ± 0.05 V in $CH_2Cl_2$, with a small but notable increase (0.11 V in both solvents) as the substituent R moves from electron donating to electron withdrawing. Values for **5d** are slightly lower than expected in both solvents, although the individual $E_m$ and $E_n$ values for **5d** still follow the expected trend.

At lower concentrations (Table 3), the potential range for the "reduction" process is from −0.57 to −0.46 V vs $Fc^{0/+}$ in $CH_3CN$ (change of 0.11 V) and −0.51 to −0.42 V vs $Fc^{0/+}$ in $CH_2Cl_2$ (change of 0.09 V). The potential range for the irreversible "oxidation" process is from 0.59 to 0.84 V vs $Fc^{0/+}$ in $CH_3CN$ and 0.66 to 0.91 V vs $Fc^{0/+}$ in $CH_2Cl_2$ for an overall change of 0.25 V in both solvents. Average $E_{cell}$ values (where $E_{cell} = E_p^{a2} - E_p^{a1}$) are 1.20 ± 0.05 V in $CH_3CN$ and 1.21 ± 0.06 V in $CH_2Cl_2$, which are essentially identical for both solvents. This contrasts with the small but notable change in $E_{cell}$ values (~100 mV) at higher concentrations between the two solvents. For a monomeric neutral thiatriazinyl radical, the redox process is assumed to involve removal from or addition to the $\pi$-SOMO and can be represented as

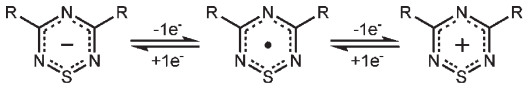


[1]

Since the same redox orbital is involved in the electrochemical oxidation and reduction reactions, one expects the substituents R to influence both redox processes by the same amount, so long as the influence is purely inductive. Exactly this has been observed in electrochemical investigations of more than 20 1,2,3,5-dithiadiazolyls.[3] However, unlike the dithiadiazolyls, the redox orbital of the thiatriazinyls (the SOMO, Figure 10) does not have a node at the substituent-bearing carbon atoms. It is to be expected, therefore, that resonance effects can have a significant influence. These are expected to affect the oxidation and reduction processes differently.

Another factor that cannot be discounted is the effect of dimer formation on the redox processes since thiatriazinyls form strong


dx.doi.org/10.1021/ic2003996 |Inorg. Chem. 2011, 50, 5123–5136

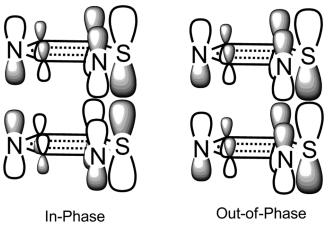


**Figure 12.** The in-phase and out-of-phase combinations of the $3b_1$ SOMO of model 3,5-dihydro-1,2,4,6-thiatriazinyls.

dimers ($d$(S···S = 2.643(21) Å) compared to 1,2,3,5-dithiadiazolyls (mean $d$(S···S = 3.03−3.16 Å).[3c,22] In a dimeric thiatriazine, the redox process can be represented as

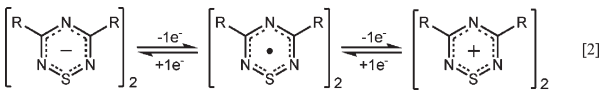


[2]

The formation of thiatriazinyl dimers has been convincingly interpreted as the result of diffuse side-on overlap of the $3b_1$ $\pi$ orbital of the individual thiatriazinyl rings (Figure 12) in a face-to-face dimeric arrangement similar to that found in the solid state for dithionite salts.[5e,23] This overlap represents the only net "bonding" interaction between the rings; that it is centered on a single sulfur atom which has the largest share of the unpaired spin density leads to relatively strong bonding. The dimer is a diamagnetic species, and hence oxidation occurs from a different orbital (the in-phase combination) than reduction (the out-of-phase combination). It is therefore to be expected that the substituents influence these distinct orbitals by different amounts.

**Digital Modeling of CVs of the 1,2,4,6-Thiatriazinyls.** In order to further probe the effect of monomer−dimer equilibrium on the voltammetry, we turned to digital modeling of the voltammograms at both low and high concentrations using DigiElch software.[24] Starting with lower concentrations of the radical in solution (~1/10 the values listed in Table 2), we established a plausible model for the monomer undergoing both a chemically irreversible oxidation and a reversible reduction. The resultant CV is shown as the blue trace in Figure 13. In this case, the model assumes that following a one-electron oxidation of the thiatriazinyl radical (abbreviated as $[TTA]^{\bullet}$ in Scheme 2) there is a chemically irreversible first-order decay step ($K_{eq\ 4}$= $10^6$, $k_{f4}$ = 5 $s^{-1}$). No chemical step is associated with the one-electron reduction. Then, at higher concentrations, the model which fit most closely to the experimental CVs follows the "ladder" scheme shown in Scheme 2.[25] The favorable formation of the dimer $[TTA_2]$ at higher concentrations ($K_{eq\ 1}$ = 400−800, $k_{f1}$ = 1 $M^{-1}$ $s^{-1}$) and the unfavorable formation of the dication dimer $[TTA_2]^{2+}$ ($K_{eq\ 2}$ < 1, $k_{f2}$ = 0.01 $M^{-1}$ $s^{-1}$) results in very satisfactory simulations (they are a good visual match to experimental data, see black trace in Figure 13) when the oxidation of the $[TTA_2]$ dimer is a two-electron process. Assuming a one-electron oxidation for this step does not result in a good match. The formation of the monoanionic dimer $[TTA_2]^{\bullet-}$ from $[TTA]^{\bullet}$ + $[TTA]^{-}$ was also favored ($K_{eq\ 3}$ = 271, $k_{f3}$ < 10 $M^{-1}$ $s^{-1}$).

The value for $K_{eq\ 1}$ of 400−800 is in reasonable agreement with previously derived equilibrium constants for the association of diphenyl thiatriazinyls and selenatriazinyls from Oakley et al. from EPR experiments ($K_{eq}$ = 33 for sulfur and $K_{eq}$ = 2000 for selenium).[6] Similar investigations into the monomer−dimer equilibrium for 4-(2′-pyridyl)-1,2,3,5-dithiadiazolyl ($K_{eq} \cong$ 0.05 at RT)

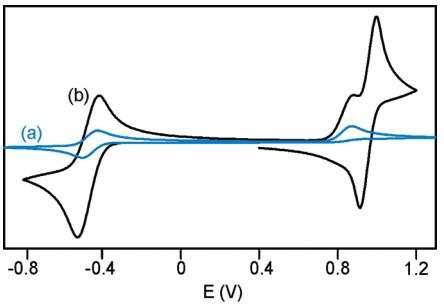


**Figure 13.** Calculated CVs for both (a) monomeric (blue line) and (b) dimeric (black line) solutions of **5e** resulting from the input of kinetic parameters listed in the text and following the "ladder" scheme shown in Scheme 2. These CVs follow the specific case of $\nu$ = 0.2 V $s^{-1}$, $K_{eq\ 1}$ = 400, $k_{f1}$ = 1 $M^{-1}$ $s^{-1}$, $K_{eq\ 2}$ = 0.0766, $k_{f2}$ = 0.01 $M^{-1}$ $s^{-1}$, $K_{eq\ 3}$ = 271, $k_{f3}$ = 1 $M^{-1}$ $s^{-1}$, $K_{eq\ 4}$ = $10^6$, $k_{f4}$ = 5 $s^{-1}$ (first-order decay of $[TTA]^{+}$), $k_{s1}$ = $k_{s2}$ = $k_{s3}$ = $k_{s4}$ = 0.03 cm $s^{-1}$, conc. dimer =0.01 mol $L^{-1}$, conc. monomer 0.001 mol $L^{-1}$. The potential was first swept in the cathodic direction starting from 0.4 V.

**Scheme 2. Proposed "Ladder" Scheme Interrelating the Voltammetric Behavior of Thiatriazinyls at Lower and Higher Concentrations**

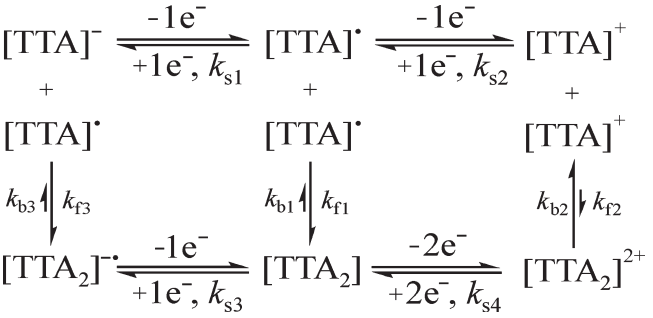


have been undertaken using absorption spectroscopy.[2e] The self-consistent fit of these data to the "ladder" scheme is thus satisfying and chemically reasonable in view of the large association constants expected for thiatriazinyls. That the dication favors monomers fits well with removal of the very electrons involved in the association. The only surprise is the apparent "decomposition" of the monomeric cation under inert conditions where these 6$\pi$ Hückel species are expected to be thermally stable.[5i] We propose that the irreversibility of this electrode process may involve electron self-exchange.[26] Thus, a rapid pseudo-first-order cascade reaction:

$$[TTA]^{+} + [TTA]^{\bullet} \leftrightarrow [TTA]^{\bullet} + [TTA]^{+} \qquad (3)$$

could remove the cation from the electrode surface when the dominant species in solution is $[TTA]^{\bullet}$. On the other hand, when $[TTA_2]$ is the dominant species, the driving force for the self-exchange reaction weakens, and this reaction may become sluggish. While we believe that this mechanism is a plausible proposal, detailed testing in which actual voltammograms are fit to theory will be required to obtain precise values for the kinetic parameters. Such an undertaking is beyond the scope of the current project.

**Correlation of Redox Potentials with Gas Phase Calculations.** Previous studies have shown that quantum calculations, when used judiciously, can provide corroboration of electrochemical results.[3] Fully geometry optimized calculations at the (U)B3LYP/6-31G(d) level of theory were performed for the


dx.doi.org/10.1021/ic2003996 |Inorg. Chem. 2011, 50, 5123–5136

**Table 4. Calculated and Experimental Redox Potentials of 5a−e for the Monomeric Radical**

| | −1/0 process | | | 0/+1 process | | |
|---|---|---|---|---|---|---|
| | | $E_m$ (V) | $E_m$ (V) | | $E_p^{a1}$ (V) | $E_p^{a1}$ (V) |
| cmpd | calc (eV) | $CH_3CN$ | $CH_2Cl_2$ | calc (eV) | $CH_3CN$ | $CH_2Cl_2$ |
| **5a** | −1.89 | −0.57 | −0.51 | 7.29 | 0.59 | 0.66 |
| **5b** | −1.94 | −0.56 | −0.50 | 7.50 | 0.67 | 0.71 |
| **5c** | −1.99 | −0.54 | −0.48 | 7.65 | 0.73 | 0.76 |
| **5d** | −2.16 | −0.50 | −0.46 | 7.72 | 0.74 | 0.81 |
| **5e** | −2.25 | −0.46 | −0.42 | 7.90 | 0.84 | 0.91 |
| Δ | 0.36 | 0.11 | 0.09 | 0.61 | 0.25 | 0.25 |

monomeric cation, anion, and neutral thiatriazine derivatives. No attempt was made to model the weakly bound dimeric molecules. The energies of these optimized molecules were then used to define the theoretical redox reactions:

$$0/+1 \text{ process} : E_{cation} - E_{radical} = E_{oxidation} \quad (4)$$

$$-1/0 \text{ process} : E_{anion} - E_{radical} = E_{reduction} \quad (5)$$

Table 4 lists the calculated and experimental redox potentials for **5a−e** from the experimental CV data at low concentrations taken from Table 3, and correlation curves are presented in Figure 14. The results are graphed by process type, and each graph includes results for both solvents.

Excellent correlation is obtained between the calculated gas phase and experimental solution phase oxidation and reduction potentials of the monomeric radicals **5a−e**, which is particularly noteworthy for the 0/+1 process, which uses peak potentials from an irreversible process in both solvents.[3b] The reliability of the electrochemical data for this series obtained from CV is confirmed by this correlation. The solution oxidation and reduction potentials also correlate well with Hammett $\sigma_p$ substituent constants (Figures S22 and S23, Supporting Information).[27]

## CONCLUSIONS

This paper reports a comprehensive investigation of a complete series of unsymmetrical aryl/trifluoromethyl-substituted thiatriazinyls. The synthetic work has elaborated new and versatile imidoylamidine reagents and demonstrated their ability to form the ring compounds through direct condensation with sulfur halides. Conversion to the neutral thiatriazinyls was successful for all five exemplars. All of the synthetic results are supported by thorough structural studies that provide extremely reliable mean parameters from high-quality, low-temperature diffraction data. The complex EPR spectral data are shown to fit to well-defined substituent trends even though the variation in hfs values is small. Finally, complex voltammetric behavior involving the first reliably detected monomer−dimer equilibria in the history of the electrochemistry of thiazyl rings has been modeled using sophisticated digital software to provide a interpretation that is consistent with the predicted chemical nature of the various redox products. Further work on thiatriazinyls including detailed fitting of monomer−dimer equilibria to voltammetric data is in progress in our laboratory and will be reported at a future time.

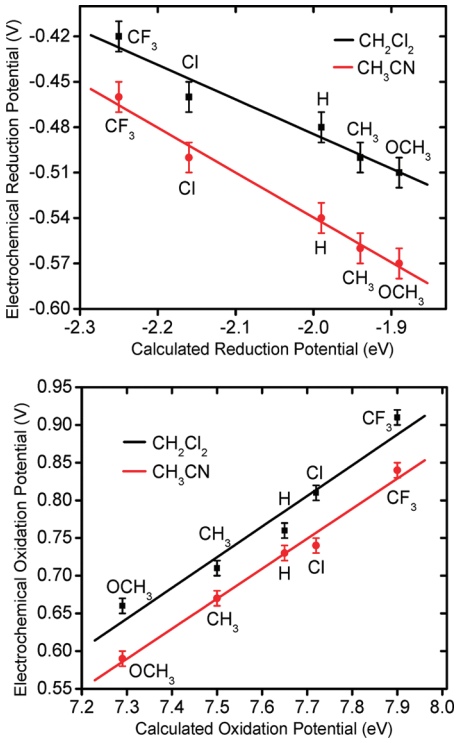


**Figure 14.** Plot of the calculated vs experimental monomer reduction potentials (top) and oxidation potentials (bottom) of **5a−e** as measured by cyclic voltammetry in $CH_2Cl_2$ (black line, $R = 0.975$, top; $R = 0.975$, bottom), and (b) $CH_3CN$ (red line, $R = 0.993$, top; $R = 0.994$, bottom) solution. Error bars express an estimated error in measured potential of ±0.01 V.

## EXPERIMENTAL SECTION

**General Procedures.** Trifluoroacetonitrile (PCR Inc.) was obtained commercially and used as received. $SCl_2$ (Aldrich) was distilled from $PCl_3$ with $CaCl_2$ moisture protection. Triphenylantimony (Aldrich) and HCl(g) (Praxair) were obtained commercially and used as received. The substituted aryl amidine hydrochlorides were prepared according to the literature method.[7] Unless otherwise indicated, all procedures were performed under an atmosphere of purified $N_2$ using a drybox, Schlenkware, and vacuum-line techniques. Solvents used were reagent-grade or better. Acetonitrile (HPLC grade) was double-distilled from $P_2O_5$ and $CaH_2$. Dichloromethane was distilled from $CaH_2$. *n*-Heptane was dried by distillation over $LiAlH_4$ and toluene over sodium. Anhydrous diethyl ether was dried by distillation from sodium wire.

**Spectroscopic Methods.** Infrared spectra were obtained as KBr plates and were recorded on a Bomem MB102 Fourier transform spectrometer. Melting points were determined on an electrothermal melting point apparatus (capillaries) and are uncorrected. EPR spectra (X band) were recorded on a Bruker EMX-113/12 spectrometer as solutions in dichloromethane in 4 mm Pyrex glass tubes sealed under vacuum conditions. NMR spectra were acquired at 250.13 ($^1$H) and 62.90 ($^{13}$C) MHz on a Bruker/Tecmag AC250 spectrometer using $CDCl_3$ as the solvent and thus a reference. Mass spectra were recorded by the Mass Spectrometry Center, University of Alberta, Edmonton. Microanalyses were performed by M−H−W Laboratories in Phoenix, Arizona.

**Electrochemical Methods and Procedures.** Crystals of high purity **5a−e** were collected, weighed, and loaded into individual break-seal tubes and attached to the electrochemical cell by fusing the glass along with a known mass of ferrocene in a separate break-seal.[25] The electrodes are all platinum and were sealed into the glass and cleaned in


dx.doi.org/10.1021/ic2003996 |*Inorg. Chem.* 2011, 50, 5123–5136

between experiments using concentrated $HNO_3$. Cyclic voltammograms (CVs) were obtained at temperatures of 21 ± 2 °C in $CH_3CN$ and $CH_2Cl_2$ solutions containing 0.1 and 0.4 M [$^nBu_4N$][$PF_6$], respectively, as the supporting electrolyte. The electrolyte was loaded into the cell and dried under vacuum conditions in an oil bath set at 80 °C overnight prior to transfer of the solvent. Both $CH_2Cl_2$ and $CH_3CN$ were distilled and stored over molecular sieves prior to use. The solvents were freeze−thaw−degassed at least five times prior to their transfer into the cell over a vacuum line. For CVs, all measurements were recorded at room temperature (22 ± 2 °C), and the scan rates were varied between 0.1 and 10 V $s^{-1}$.

In a typical experiment, the electrolyte solution is scanned to obtain a background current and determine the effective electrochemical window. Next, the seal to the analyte is broken, and a small amount is dissolved until a signal with satisfactory S/N is obtained. The concentration of the analyte is incrementally increased while obtaining CV traces. Finally, all of the analyte is thoroughly mixed with the electrolyte solution to establish a known "full" concentration. After all CV data are satisfactorily recorded, the seal to the reference is broken, and a sufficient quantity of ferrocene is added to the cell to obtain an accurate reference for the voltage scale.

**X-Ray Crystallography.** Crystals were selected and mounted in Paratone on the ends of thin glass capillaries and cooled on the goniometer head to −100 °C with the Bruker low-temperature accessory attached to the APPEX-II diffractometer. Mo Kα radiation ($\lambda$ = 0.71073 Å) was used throughout. Multiscan absorption corrections were applied to all of the data sets, and refinement was conducted with full-matrix least-squares on $F^2$ using SHELXTL 6.14.[28] In the case of **5b**, data sets collected at −100 °C solve and refine but are stuck at $R_1$ = 0.14 due to a suspected superlattice formation. Therefore, another crystal was selected, covered in epoxy cement, and glued to the end of a glass fiber. Diffraction data collected at 23 °C refined to a low R factor and provided a fully acceptable structure. Details of the refinements and disorder models for typical rotational disorder of $CF_3$ groups are provided in the electronic crystallographic information file. Crystal data and refinement parameters are also summarized in Table 5. Structures of **2c** and **5c** were determined at room temperature and at −100 °C.

**Computational Details.** DFT calculations undertaken for this study employed geometry optimization at the (U)B3LYP/6-31G(d) level. Harmonic vibrational frequencies were calculated for all optimized geometries to confirm that they are stationary points. Calculations of energies and EPR hyperfine splitting (hfs) constants used the same level of theory. All calculations were performed using the Gaussian 98 suite of programs.[18]

**Synthesis of Amidines 1a−e.** $C_6H_4C(NH)NH_2$, **1c**. Benzamidine hydrochloride hydrate (26.3 g, 0.173 mol) and KOH (32.4 g, 0.576 mol) were added to 175 mL of distilled water. $CH_2Cl_2$ (2 × 200 mL) was used to extract the product. The solvent was rotary evaporated, leaving a pale yellow oil which solidified overnight in the freezer. The solid was sublimed at 80 °C under vacuum conditions to give 12.79 g (61.9% yield) of pure white **1c**. $^1$H NMR ($CDCl_3$): $\delta$ 5.28 (s, 3H, NH), 7.42−7.62 (m, 5H, phenyl).

$CH_3OC_6H_4C(NH)NH_2$, **1a**. 4-Methoxybenzonitrile (15.08 g, 0.1133 mol) was added to $Et_2O\cdot LiN(SiMe_3)_2$ (27.26 g, 0.1129 mol) in 200 mL of distilled diethyl ether and stirred for 20 h with a drying tube attached. A 1:1 mixture of ethanol and concentrated HCl (30 mL) was added slowly through a dropping funnel, leaving a white precipitate. The solid was recovered by filtration and dried in the air. It was then redissolved in distilled water and treated with excess NaOH solution, affording a pale purple solid. This was sublimed at 91 °C under vacuum conditions to give 3.72 g (22.2% yield) of pure **1a**. Plate-shaped X-ray-quality crystals were collected on a coldfinger following vacuum sublimation. $^1$H NMR ($CDCl_3$): $\delta$ 3.85 (s, 3H, $CH_3$), 4.99 (s, 3H, NH), 6.93 (d, 2H, $J_{H-H}$ = 9.0 Hz, $C_{Ar}H$), 7.57 (d, 2H, $J_{H-H}$ = 8.4 Hz, $C_{Ar}H$).

$CH_3C_6H_4C(NH)NH_2$, **1b**. *p*-Tolunitrile (6.356 g, 0.05425 mol) was added to $Et_2O\cdot LiN(SiMe_3)_2$ (12.47 g, 0.05165 mol) in 200 mL of distilled diethyl ether and stirred for 22 h with a drying tube attached. A 1:1 mixture of ethanol and concentrated HCl (30 mL) was added slowly through a dropping funnel to give a pink precipitate. The solid was recovered by filtration and dried in the air. It was then redissolved in distilled water and treated with excess KOH. $CH_2Cl_2$ (2 × 200 mL) was used to extract the product. The solvent was rotary evaporated, and the solution was dried using andrydrous sodium sulfate to give a yellow solid. The solid was sublimed at 70 °C under vacuum conditions to give 1.51 g (21.8% yield) of pure **1b**. $^1$H NMR ($CDCl_3$): $\delta$ 2.40 (s, 3H, $CH_3$), 4.83 (s, 3H, NH), 7.23 (d, 2H, $J_{H-H}$ = 8.1 Hz, $C_{Ar}H$), and 7.51 (d, 2H, $J_{H-H}$ = 8.4 Hz, $C_{Ar}H$).

$ClC_6H_4C(NH)NH_2$, **1d**. Amidine **1d** was prepared by the same method reported for **1a** using 4-chlorobenzonitrile (7.69 g, 0.0559 mol) and $Et_2O\cdot LiN(SiMe_3)_2$ (12.7 g, 0.0524 mol) in 200 mL of distilled diethyl ether. The pale pink-colored solid was sublimed at 91 °C under vacuum conditions to give 4.33 g (53.7% yield) of pure **1d**. $^1$H NMR ($CDCl_3$): $\delta$ 3.88 (s, 3H, NH), 7.41 (d, 2H, $J_{H-H}$ = 8.4 Hz, $C_{Ar}H$), and 7.75 (d, 2H, $J_{H-H}$ = 8.7 Hz, $C_{Ar}H$).

$CF_3C_6H_4C(NH)NH_2$, **1e**. Amidine **1e** was prepared by the same method reported for **1a** using α,α,α-trifluoro-*p*-tolunitrile (8.94 g, 52.2 mmol) and $Et_2O\cdot LiN(SiMe_3)_2$ (12.4 g, 51.5 mmol) in 200 mL of distilled diethyl ether. After the solid was collected by filtration and air-dried, it was sublimed at 85 °C under vacuum conditions to give 5.61 g (57.9% yield) of pure **1e**. $^1$H NMR ($CDCl_3$): $\delta$ 4.90 (s, 3H, NH), 7.75 (d, 2H, $J_{H-H}$ = 8.4 Hz, $C_{Ar}H$), 7.70 (d, 2H, $J_{H-H}$ = 8.4 Hz, $C_{Ar}H$). $^{19}$F NMR ($CDCl_3$): $\delta$ −62.02 ($CF_3$).

**Synthesis of Trifluoromethyl Imidoylamidines 2a−e.** $C_6H_5C_3N_3H_3F_3$, **2c**. Trifluoroacetonitrile (2.06 g, 21.7 mmol) was measured on a vacuum line by PVT methods and added to 2.53 g (21.1 mmol) of benzamidine **1c** in 20 mL of acetonitrile in a 300 × 25 mm heavy-wall Pyrex reactor fitted with a Rotaflow stopcock equipped with a small magnetic stirring bar at −196 °C. The mixture was warmed to RT, heated to 60 °C with stirring for 10 min, and then cooled to RT and evaporated, leaving a clear oil. Upon refrigeration, this solidified to leave 4.37 g of a white solid (20.3 mmol, 96% yield), mp 42−45 °C. $^1$H NMR ($\delta$, $CDCl_3$): 6.8 (s, NH), 7.38−7.54 (m, 3H, phenyl), 7.83−7.88 (m, 2H, $C_{Ar}H$), 9.1 (s, NH), 11.0 (s, NH). $^{13}$C NMR ($\delta$, $CDCl_3$): 117.8 (q, 281 Hz), 127.4 (s), 129.0 (s), 132.2 (s), 135.2 (s), 163.5 (q, 33 Hz), 165.9 (s). Mass spectrum (*m*/*e*): 214 ($PhC_2N_3H_2CF_3^+$, 100%), 169 ($PhC_2N_2H_2F_2^+$, 4%), 146 ($PhC_2N_3H_3^+$, 12%), 129 ($PhC_2N_2^+$, 6%), 104 ($PhCNH^+$, 48%). Analysis calculated (found): 50.24 (50.35)% C, 3.75 (4.01)% H, 19.53 (19.37)% N.

4-$CH_3OC_6H_5C_2N_3H_3CF_3$, **2a**. Imidoylamidine **2a** was prepared by the same method as **2c** using $CF_3CN$ (1.09 g, 11.5 mmol) and **1a** (1.58 g, 10.5 mmol) in 10 mL of acetonitrile. A white solid remained, which was sublimed *in vacuo* at 46 °C to leave 1.43 g of pure white crystals (5.8 mmol, 56% yield), mp 41−45 °C. $^1$H NMR ($\delta$, $CDCl_3$): 3.9 (s, $OCH_3$), 6.7 (s, NH), 6.9 (d, 2H, $C_{Ar}H$), 7.9 (d, 2H, $C_{Ar}H$), 9.0 (s, NH), 11.0 (s, NH). $^{13}$C NMR ($\delta$, $CDCl_3$): 55.7 (s), 114.3 (s), 117.9 (q, 281 Hz), 127.3 (s), 129.3 (s), 163.1 (s), 163.4 (q, 33 Hz), 165.3 (s). Mass spectrum (*m*/*e*): 244 ($CH_3OPhC_2N_3H_2CF_3^+$, 42%), 199 ($CH_3OPhC_2N_2H_2F_2^+$, 4%), 176 ($CH_3OPhC_2N_3H_3^+$, 20%), 159 ($CH_3OPhC_2N_2^+$, 13%), 134 ($CH_3OPhCNH^+$, 100%). Analysis calculated (found): 48.98 (48.85)% C, 4.11 (4.22)% H, 17.14 (17.32)% N.

4-$CH_3C_6H_5C_2N_3H_3CF_3$, **2b**. Imidoylamidine **2b** was prepared by the same method as **2c** using $CF_3CN$ (1.34 g, 14.1 mmol) and **1b** (1.96 g, 14.6 mmol) in 15 mL of acetonitrile. A pink solid remained, which was sublimed in vacuo at 48 °C to leave 2.48 g of white crystals (10.8 mmol, 77% yield), mp 54−57 °C. $^1$H NMR ($\delta$, $CDCl_3$): 2.4 (s, $CH_3$), 6.7 (s, NH), 7.3 (d, 2H, $C_{Ar}H$), 7.8 (d, 2H, $C_{Ar}H$), 9.1 (s, NH), 11.0 (s, NH). $^{13}$C NMR ($\delta$, $CDCl_3$): 21.7 (s), 117.8 (q, 281 Hz), 127.6 (s), 129.7 (s), 132.4 (s), 142.8 (s), 163.6 (q, 33 Hz), 165.8 (s). Mass spectrum (*m*/*e*): 228 ($CH_3PhC_2N_3H_2CF_3^+$, 100%), 183 ($CH_3PhC_2N_2H_2F_2^+$, 2%), 160 ($CH_3PhC_2N_3H_3^+$, 7%), 143 ($CH_3PhC_2N_2^+$, 4%), 118 ($CH_3PhCNH^+$, 30%). Analysis calculated (found): 52.40 (52.34)% C, 4.40 (4.60)% H, 18.33 (18.50)% N.


dx.doi.org/10.1021/ic2003996 |*Inorg. Chem.* 2011, 50, 5123–5136

**Table 5. Crystallographic Data and Refinement Parameters for Compounds 1−6**

| complex | 1a | 2a | 2c | 2e | 4b | 4e |
|---|---|---|---|---|---|---|
| empirical formula | $C_8H_{10}N_2O$ | $C_{10}H_{10}F_3N_3O$ | $C_9H_8F_3N_3$ | $C_{10}H_7F_6N_3$ | $C_{10}H_7ClF_3N_3S$ | $C_{10}H_4ClF_6N_3S$ |
| $M_r$ | 150.18 | 245.21 | 215.18 | 283.19 | 293.70 | 347.67 |
| cryst size ($mm^3$) | 0.25 × 0.15 × 0.12 | 0.45 × 0.37 × 0.20 | 0.401 × 0.208 × 0.116 | 0.652 × 0.429 × 0.310 | 0.31 × 0.16 × 0.16 | 0.17 × 0.14 × 0.14 |
| cryst syst | triclinic | triclinic | monoclinic | monoclinic | orthorhombic | monoclinic |
| space group | $P\bar{1}$ | $P\bar{1}$ | $P2_1/n$ | $P2_1/n$ | $P2_12_12$ | $P2_1/c$ |
| $a$ (Å) | 5.005(10) | 9.2967(19) | 8.8135(17) | 11.2481(8) | 14.507(3) | 14.5920(14) |
| $b$ (Å) | 10.15(2) | 10.538(2) | 16.356(3) | 14.6690(10) | 17.395(3) | 11.8343(11) |
| $c$ (Å) | 15.54(3) | 11.787(3) | 14.069(3) | 14.3328(10) | 4.7852(8) | 7.4331(7) |
| α (deg) | 86.58(2) | 93.783(2) | 90.00 | 90.00 | 90.00 | 90.00 |
| $\beta$ (deg) | 87.40(2) | 105.567(2) | 101.503(2) | 93.7750(10) | 90.00 | 94.7720(10) |
| $\gamma$ (deg) | 79.77(2) | 97.335(2) | 90.00 | 90.00 | 90.00 | 90.00 |
| $V$ ($Å^3$) | 775(3) | 1097.2(4) | 1987.3(7) | 2359.8(3) | 1207.6(3) | 1279.1(2) |
| $Z$ | 4 | 4 | 8 | 8 | 4 | 4 |
| $D_c$ ($Mg\cdot m^{-3}$) | 1.287 | 1.484 | 1.438 | 1.594 | 1.615 | 1.805 |
| $\mu$ ($mm^{-1}$) | 0.088 | 0.134 | 0.130 | 0.165 | 0.511 | 0.530 |
| $\theta$ range | 2.04−27.89 | 1.80−27.00 | 1.93−27.42 | 1.99−26.36 | 1.83−29.59 | 2.22−28.83 |
| coll. reflns | 8956 | 12270 | 28147 | 24664 | 12307 | 14808 |
| obsd reflns | 3580 | 4750 | 4532 | 4826 | 2987 | 3137 |
| no. of params | 219 | 333 | 345 | 404 | 192 | 217 |
| $F$(000) | 320 | 504 | 880 | 1136 | 592 | 688 |
| $T$ (K) | 173(2) | 173 (2) | 173(2) | 173(2) | 173(2) | 173(2) |
| R1, wR2 [$I > \sigma 2(I)$] | 0.0410, 0.0959 | 0.0338, 0.0842 | 0.0370, 0.0859 | 0.0468, 0.1217 | 0.0379, 0.0965 | 0.0327, 0.0843 |
| R1, wR2 [all data] | 0.0695, 0.1053 | 0.0420, 0.0896 | 0.0496, 0.0934 | 0.0538, 0.1298 | 0.0550, 0.1026 | 0.0414, 0.0895 |
| GOF | 0.978 | 1.038 | 1.041 | 1.038 | 1.031 | 1.056 |

| complex | 5a | 5b | 5c | 5d | 5e | 6 |
|---|---|---|---|---|---|---|
| empirical formula | $C_{10}H_7F_3N_3OS$ | $C_{10}H_7F_3N_3S$ | $C_9H_5F_3N_3S$ | $C_9H_4ClF_3N_3S$ | $C_{10}H_4F_6N_3S$ | $C_7H_7ClN_2O_2S$ |
| $M_r$ | 274.25 | 258.25 | 244.22 | 278.66 | 312.22 | 218.66 |
| Cryst size ($mm^3$) | 0.476 × 0.192 × 0.118 | 0.185 × 0.171 × 0.153 | 0.287 × 0.215 × 0.086 | 0.29 × 0.22 × 0.14 | 0.311 × 0.155 × 0.06 | 0.13 × 0.12 × 0.12 |
| cryst syst | triclinic | triclinic | triclinic | triclinic | triclinic | tetragonal |
| space group | $P\bar{1}$ | $P\bar{1}$ | $P\bar{1}$ | $P\bar{1}$ | $P\bar{1}$ | $P4_12_12$ |
| $a$ (Å) | 7.1075(8) | 11.5126(12) | 9.136(4) | 11.1851(15) | 10.7943(6) | 9.4879(9) |
| $b$ (Å) | 11.5130(13) | 14.7539(15) | 10.728(4) | 14.799(2) | 13.3162(8) | 9.4879(9) |
| $c$ (Å) | 13.3832(15) | 15.0498(15) | 11.016(5) | 14.806(2) | 16.7910(10) | 21.584(4) |
| α (deg) | 88.0000(10) | 111.2160(10) | 84.652(4) | 110.9450(10) | 94.0420(10) | 90.00 |
| $\beta$ (deg) | 86.2810(10) | 99.9130(10) | 69.663(4) | 103.210(2) | 107.4760(10) | 90.00 |
| $\gamma$ (deg) | 80.4830(10) | 107.6770(10) | 68.715(3) | 106.5720(10) | 96.1190(10) | 90.00 |
| $V$ ($Å^3$) | 1077.5(2) | 2153.0(4) | 942.6(7) | 2038.8(5) | 2275.6(2) | 1943.0(5) |
| $Z$ | 4 | 8 | 4 | 8 | 8 | 8 |
| $D_c$ ($Mg\cdot m^{-3}$) | 1.691 | 1.593 | 1.721 | 1.816 | 1.823 | 1.495 |
| $\mu$ ($mm^{-1}$) | 0.333 | 0.321 | 0.362 | 0.600 | 0.358 | 0.576 |
| $\theta$ range | 1.79−27.42 | 1.96−26.59 | 1.97−27.45 | 1.61−28.49 | 1.90−28.73 | 2.34−26.86 |
| coll. reflns | 15562 | 23211 | 13575 | 22885 | 26627 | 21297 |
| obsd reflns | 4872 | 8841 | 4267 | 9467 | 10697 | 2076 |
| no. of params | 327 | 729 | 577 | 629 | 777 | 124 |
| $F$(000) | 556 | 1048 | 492 | 1112 | 1240 | 896 |
| $T$ (K) | 173(2) | 296(2) | 173(2) | 173(2) | 173(2) | 173(2) |
| R1, wR2 [$I > \sigma 2(I)$][a,b] | 0.0273, 0.0732 | 0.0379, 0.1035 | 0.0368, 0.0976 | 0.0426, 0.0893 | 0.0440, 0.1137 | 0.0421, 0.1102 |
| R1, wR2 [all data][a,b] | 0.0302, 0.0757 | 0.0572, 0.1127 | 0.0444, 0.1036 | 0.0825, 0.1054 | 0.0689, 0.1256 | 0.0610, 0.1166 |
| GOF[c] | 1.032 | 1.026 | 1.047 | 1.022 | 1.036 | 0.984 |

[a] wR2 = $[\Sigma\{w(F_o^2 - F_c^2)^2\}/\Sigma w (F_o^2)^2]^{1/2}$; R1 = $\Sigma||F_o| - |F_c||/\Sigma|F_o|$. [b] $F_o > 4\sigma(F_o)$. [c] GOF = $[\Sigma\{w (F_o^2 - F_c^2)^2\}/(n - p)]^{1/2}$, where $n$ = number of reflections and $p$ = number of refined parameters.

4-$ClC_6H_5C_2N_3H_3CF_3$, **2d**. Imidoylamidine **2c** was prepared by the same method as **2c** using trifluoroacetonitrile (2.07 g, 21.8 mmol) and **1d** (3.25 g, 21.0 mmol) in 20 mL of acetonitrile. A white solid remained which was sublimed *in vacuo* at 49 °C to leave 4.72 g of pure white crystals (18.9 mmol, 90% yield), mp 45−48 °C. $^1$H NMR ($\delta$, $CDCl_3$): 6.7 (s, NH), 7.4 (d, 2H, $C_{Ar}H$), 7.8 (d, 2H, $C_{Ar}H$), 9.2 (s, NH), 11.0


dx.doi.org/10.1021/ic2003996 |*Inorg. Chem.* 2011, 50, 5123–5136

(s, NH). $^{13}$C NMR ($\delta$, $CDCl_3$): 117.7 (q, 281 Hz), 128.8 (s), 129.3 (s), 133.6 (s), 138.6 (s), 163.3 (q, 34 Hz), 164.8 (s). Mass spectrum ($m/e$): 248 ($ClPhC_2N_3H_2CF_3^+$, 42%), 180 ($ClPhC_2N_3H_3^+$, 10%), 163 ($ClPhC_2N_2^+$, 13%), 138 ($ClPhCNH^+$, 100%). Analysis calculated (found): 43.31 (43.50)% C, 2.83 (3.00)% H, 16.83 (17.06)% N.

4-$CF_3C_6H_5C_2N_3H_3CF_3$, **2e**. Imidoylamidine **2e** was prepared by the same method as **2c** using trifluoroacetonitrile (1.02 g, 10.7 mmol) and **1e** (1.98 g, 10.5 mmol) in 10 mL of acetonitrile. A white solid remained which was sublimed *in vacuo* at 60 °C to leave 2.52 g of white crystals (8.9 mmol, 85% yield), mp 80−83 °C. $^1$H NMR ($\delta$, $CDCl_3$): 6.8 (s, NH), 7.7 (d, 2H, $C_{Ar}H$), 8.0 (d, 2H, $C_{Ar}H$), 9.3 (s, NH), 11.1 (s, NH). $^{13}$C NMR ($\delta$, $CDCl_3$): 117.7 (q, 281 Hz), 123.9 (q, 273 Hz), 126.0 (q, 4 Hz), 127.9 (s), 133.9 (q, 33 Hz), 138.6 (s), 163.2 (q, 34 Hz), 164.7 (s). Mass spectrum ($m/e$): 282 ($CF_3PhC_2N_3H_2CF_3^+$, 100%), 237 ($CF_3PhC_2N_2H_2F_2^+$, 5%), 214 ($CF_3PhC_2N_3H_3^+$, 13%), 197 ($CF_3PhC_2N_2^+$, 3%), 172 ($CF_3PhCNH^+$, 45%). Analysis calculated (found): 42.42 (42.32)% C, 2.49 (2.39)% H, 14.84 (14.88)% N.

**Synthesis of Trifluoromethyl Imidoylamidine Hydrochlorides 3a−e.** $C_6H_5C_3N_3H_3F_3\cdot HCl$, **3c**. Anhydrous HCl was bubbled through a suspension of **2c** (2.04 g, 9.5 mmol) in diethyl ether. The white precipitate was filtered in the air and dried to leave 2.34 g of crude solid (9.3 mmol, 98% yield), mp (dec.) 174−175 °C. For FTIR data, see the Supporting Information.

4-$CH_3OC_6H_4C_3N_3H_3F_3\cdot HCl$, **3a**. Imidoylamidine hydrochloride **3a** was prepared using the same method as **3c** from **2a** (1.01 g, 4.1 mmol), providing 1.09 g of a crude white solid (3.9 mmol, 94% yield), mp (dec.) 213−215 °C.

4-$CH_3C_6H_4C_3N_3H_3F_3\cdot HCl$, **3b**. Imidoylamidine hydrochloride **3b** was prepared using the same method as **3c** from **2b** (1.59 g, 6.9 mmol), providing 1.50 g of solid **3b** (5.7 mmol, 82% yield), mp (dec.) 198−200 °C.

4-$ClC_6H_4C_3N_3H_3F_3\cdot HCl$, **3d**. Imidoylamidine hydrochloride **3d** was prepared using the same method as **3c** from **2d** (2.40 g, 9.6 mmol), providing 2.65 g of a white solid (9.3 mmol, 97% yield), mp (dec.) > 244 °C.

4-$CF_3C_6H_4C_3N_3H_3F_3\cdot HCl$, **3e**. Imidoylamidine hydrochloride **3e** was prepared using the same method as **3c** from **2e** (2.37 g, 8.4 mmol), providing 2.65 g of a white solid (8.3 mmol, 99% yield), mp (dec.) 181−183 °C.

**Synthesis of 1-Chloro-5-aryl-3-trifluoromethyl-1,2,4,6-thiatriazines 4a−e.** $C_6H_5C_2N_3SClCF_3$, **4c**. Freshly distilled $SCl_2$ (2.8 mL, 44.1 mmol) in 10 mL of acetonitrile was added dropwise to a suspension of imidoylamidine·HCl, **3c** (2.24 g, 8.9 mmol), in 30 mL of acetonitrile. The yellow mixture was heated to reflux for 1.5 h, giving an orange-red color. After filtering to remove any solids, the solvent was removed *in vacuo* to leave an orange oil (2.23 g, 8.0 mmol, 90% yield). $^1$H NMR ($\delta$, $CDCl_3$): 7.52−7.58 (m, 2H, $C_{Ar}H$), 7.67−7.74 (m, H, $C_{Ar}H$), 8.45−8.48 (m, 2H, $C_{Ar}H$).

4-$CH_3OC_6H_5C_2N_3SClCF_3$, **4a**. Compound **4a** was prepared using the same method as **4c** using $SCl_2$ (1.6 mL, 25.1 mmol) in 10 mL of acetonitrile added dropwise to **3a** (1.45 g, 5.1 mmol) in 25 mL of acetonitrile. The solvent was removed in vacuo, leaving a dark orange oil. Recrystallization with hot toluene followed by hot acetonitrile left an orange oil (1.29 g, 81% yield). $^1$H NMR ($\delta$, $CDCl_3$): 3.94 (s, $CH_3O$), 7.02 (d, 2H, $C_{Ar}H$), 8.45 (d, 2H, $C_{Ar}H$).

4-$CH_3C_6H_5C_2N_3SClCF_3$, **4b**. Compound **4b** was prepared using the same method as **4c** using $SCl_2$ (1.8 mL, 28.3 mmol) in 10 mL of acetonitrile and **3b** (1.47 g, 5.5 mmol) in 25 mL of acetonitrile. The solvent was removed in vacuo, leaving an orange-red solid (1.77 g, 97% yield). $^1$H NMR ($\delta$, $CDCl_3$): 2.49 (s, $CH_3$), 7.35 (d, 2H, $C_{Ar}H$), 8.37 (d, 2H, $C_{Ar}H$).

4-$ClC_6H_5C_2N_3SClCF_3$, **4d**. Compound **4d** was prepared using the same method as **4c** using $SCl_2$ (2.2 mL, 34.6 mmol) in 10 mL of acetonitrile and **3d** (2.54 g, 8.9 mmol) in 40 mL of acetonitrile. The solvent was removed in vacuo, leaving a dark orange oil. This was recrystallized with hot heptane to leave an orange solid (2.78 g, 99% yield). $^1$H NMR ($\delta$, $CDCl_3$): 7.53 (d, 2H, $C_{Ar}H$), 8.41 (d, 2H, $C_{Ar}H$).

4-$CF_3C_6H_5C_2N_3SClCF_3$, **4e**. Compound **4e** was prepared using the same method as **4c** using $SCl_2$ (2.2 mL, 34.6 mmol) in 10 mL of acetonitrile and **3e** (2.13 g, 6.7 mmol) in 40 mL of acetonitrile. The solvent was removed in vacuo, leaving a dark orange oil (2.50 g, 98% yield). $^1$H NMR ($\delta$, $CDCl_3$): 7.82 (d, 2H, $C_{Ar}H$), 8.59 (d, 2H, $C_{Ar}H$).

**Synthesis of 3-Trifluoromethyl-5-aryl-1,2,4,6-thiatriazinyls 5a−e.** $C_6H_5C_2N_3SCF_3$ **5c**. A pear-shaped solids addition funnel was loaded with triphenylantimony (1.42 g, 4.0 mmol) and attached to a side arm flask containing **4c** (2.23 g, 8.0 mmol) and 25 mL of acetonitrile. After degassing the solvent with three freeze−thaw cycles and warming to RT, while still under a vacuum, the $Ph_3Sb$ was added with stirring. A fine dark purple precipitate formed, and the crystals were vacuum filtered under nitrogen to give 1.14 g of crude product (4.7 mmol, 59% yield), mp. (dec.) 110−3 °C. Purification was achieved by vacuum sublimation in a three-zone tube furnace. Mass spectrum ($m/e$): 245 ($PhC_3N_3SF_3^+$, 43%), 149 ($PhCN_2S^+$, 6%), 129 ($PhC_2N_2^+$, 3%), 104 ($PhCN^+$, 100%). Analysis calculated (found): 44.26 (44.12) % C, 2.06 (2.24) %H, 17.21 (17.13) %N.

4-$CH_3OC_6H_5C_2N_3SCF_3$, **5a**. Compound **5a** was prepared using the same method as **5c** from **4a** (1.25 g, 4.0 mmol) and $Ph_3Sb$ (0.79 g, 2.2 mmol) in 20 mL of acetonitrile to give 0.41 g of dark purple solids (1.5 mmol, 37% yield), mp (dec.) 135−40 °C. Purification was achieved by vacuum sublimation in a three-zone tube furnace. Mass spectrum ($m/e$): 274 ($CH_3OPhC_3N_3SF_3^+$, 65%), 255 ($CH_3OPhC_3N_3SF_2^+$, 4%), 179 ($CH_3OPhCN_2S^+$, 3%), 117 ($CH_3OPhCN^+$, 100%). Analysis calculated (found): 43.80 (43.90)% C, 2.57 (2.71)% H, 15.32 (15.18)% N.

4-$CH_3C_6H_5C_2N_3SCF_3$, **5b**. Compound **5b** was prepared using the same method as **5c** from **4b** (1.05 g, 3.6 mmol) and $Ph_3Sb$ (0.64 g, 1.8 mmol) in 15 mL of acetonitrile to give 0.46 g of dark purple solids (1.8 mmol, 50% yield), mp (dec.) 140−2 °C. Purification was achieved by vacuum sublimation in a three-zone tube furnace. Mass spectrum ($m/e$): 258 ($CH_3PhC_3N_3SF_3^+$, 100%), 239 ($CH_3PhC_3N_3SF_2^+$, 4%), 163 ($CH_3PhCN_2S^+$, 24%), 117 ($CH_3PhCN^+$, 45%). Analysis calculated (found): 46.51 (46.67)% C, 2.73 (2.96)% H, 16.27 (16.41)% N.

4-$ClC_6H_5C_2N_3SCF_3$, **5d**. Compound **5d** was prepared using the same method as **5c** from **4d** (2.78 g, 8.9 mmol) and $Ph_3Sb$ (1.71 g, 4.8 mmol) in 30 mL of acetonitrile to give 1.36 g of dark purple solids (4.9 mmol, 55% yield), mp (dec.) 131−4 °C. Purification was achieved by vacuum sublimation in a three-zone tube furnace. Mass spectrum ($m/e$): 278 ($ClPhC_3N_3SF_3^+$, 100%), 259 ($ClPhC_3N_3SF_2^+$, 5%), 183 ($ClPhCN_2S^+$, 18%), 137 ($ClPhCN^+$, 47%). Analysis calculated (found): 38.79 (38.72)% C, 1.45 (1.41)% H, 15.08 (15.08)% N.

4-$CF_3C_6H_5C_2N_3SCF_3$, **5e**. Compound **5e** was prepared using the same method as **5c** from **4e** (2.32 g, 6.7 mmol) and $Ph_3Sb$ (1.31 g, 3.7 mmol) in 25 mL of acetonitrile to give 0.45 g of a dark purple product (1.4 mmol, 20% yield), mp (dec.) 101−5 °C. Purification was achieved by vacuum sublimation in a three-zone tube furnace. Mass spectrum ($m/e$): 312 ($CF_3PhC_3N_3SF_3^+$, 100%), 197 ($CH_3PhC_2N_2^+$, 24%), 171 ($CF_3PhCN^+$, 30%). Analysis calculated (found): 38.47 (38.52)% C, 1.29 (1.53)% H, 13.46 (13.34)% N.

**Isolation of N-Chlorosulfonyl-N,N′-benzamidine, 6.** Attempts to grow crystals of **4** by slow cooling (−30 °C) in anhydrous $CH_3CN$ were successful only for **4b** and **4e**; in the case of **4c**, colorless crystals of a hydrolysis product (**6**) were obtained, which could be identified as N-chlorosulfonyl-N,N′-benzamidine by a single-crystal X-ray diffraction structure determination. Further characterization of this material was not undertaken.

## ■ ASSOCIATED CONTENT

**Supporting Information.** Supplemental crystal structure information, a representative NMR spectrum of imidoylamidine,


dx.doi.org/10.1021/ic2003996 |*Inorg. Chem.* 2011, 50, 5123–5136

infrared spectral data, tables of hydrogen bonds, graphs showing correlation of hfs and solution redox potentials with Hammett parameters, additional EPR spectra, data from Gaussian calculations, and electronic crystallographic data in CIF format. This material is available free of charge via the Internet at http://pubs.acs.org.

## AUTHOR INFORMATION


### Corresponding Author

*Tel.: (403) 329-2045. Fax.: (403)329-2057. E-mail: boere@uleth.ca.


## ACKNOWLEDGMENT

We thank the University of Lethbridge and the Natural Sciences and Engineering Research Council of Canada for financial support of this work. Some preliminary groundwork for this project was undertaken by Russell J. Goodman. We thank Meg O'Shea for performing DFT calculations and WestGrid for access to computational facilities and Dr. Gotthelf Wolmershäuser for determining RT X-ray structures of **2c** and **5c**.

## REFERENCES


(1) (a) Chivers, T. *A Guide to Chalcogen-Nitrogen Chemistry*; World Scientific Publishing Co.: Singapore, 2005. (b) Hicks, R. G. *Stable Radicals: Fundamentals and Applied Aspects of Odd-Electron Compounds*; Wiley: New York, 2010. (c) Torroba, T. *J. Prakt. Chem.* **1999**, *341*, 99–113. (d) Lekin, K.; Winter, S. M.; Downie, L. E.; Bao, X.; Tse, J. S.; Desgreniers, S.; Secco, R. A.; Doube, P. A.; Oakley, R. T. *J. Am. Chem. Soc.* **2010**, *132*, 16212–16224. (e) Winter, S. M.; Cvrkalj, K.; Dube, P. A.; Robertson, C. M.; Probert, M. R.; Howard, J. A. K.; Oakley, R. T. *Chem. Commun.* **2009**, 7306–7308. (f) Fujita, W.; Awaga, K. *Science* **1999**, *286*, 261–262. (g) Leitch, A. A.; Oakley, R. T.; Reed, R. W.; Thompson, L. K. *Inorg. Chem.* **2007**, *46*, 6261–6270. (h) Gilroy, J. B.; Joe, B.; Lemaire, M. T.; Patrick, B. O.; Hicks, R. G. *Cryst. Eng. Comm.* **2009**, *11*, 2180–2184. (i) Decken, A.; Mailman, A.; Passmore, J. *Chem. Commun.* **2009**, 6077–6079. (j) Vasilieva, N. V.; Irtegova, I. G.; Gritsan, N. P.; Lonchakov, A. V.; Makarov, A. Y.; Shundrin, L. A.; Zibarev, A. V. *J. Phys. Org. Chem.* **2010**, *23*, 536–543. (k) Semenov, N. A.; Pushkarevsky, N. A.; Lonchakov, A. V.; Bogomyakov, A. S.; Pritchina, E. A.; Suturina, E. A.; Gritsan, N. P.; Konchenko, S. N.; Mews, R.; Ovcharenko, V. I.; Zibarev, A. V. *Inorg. Chem.* **2010**, *49*, 7558–7564. (l) Kanai, K.; Yoshida, H.; Noda, Y.; Iwasaki, A.; Suizu, R.; Tsutumi, J.; Imabayashi, H.; Ouchi, Y.; Sato, N.; Seki, K.; Awaga, K. *Phys. Chem. Chem. Phys.* **2009**, *11*, 11432–11436. (m) Cordes, A. W.; Haddon, R. C.; Oakley, R. T. *Adv. Mater.* **1994**, *6*, 798–802. (n) Cordes, A. W.; Haddon, R. C.; Oakley, R. T. *Phosphorus, Sulfur, Silicon Relat. Elem.* **2004**, *179*, 673–684. (o) Barclay, T. M.; Cordes, A. W.; Haddon, R. C.; Itkis, M. E.; Oakley, R. T.; Reed, R. W.; Zhang, H. *J. Am. Chem. Soc.* **1999**, *121*, 969–976. (p) Brusso, J. L.; Clements, O. P.; Haddon, R. C.; Itkis, M. E.; Leitch, A. A.; Oakley, R. T.; Reed, R. W.; Richardson, J. F. *J. Am. Chem. Soc.* **2004**, *126*, 8256–8265. (q) Alberola, A.; Less, R. J.; Pask, C. M.; Rawson, J. M.; Palacio, F.; Oliete, P.; Paulsen, C.; Yamaguchi, A.; Farley, R. D.; Murphy, D. M. *Angew. Chem., Int. Ed.* **2003**, *42*, 4782–4785. (r) Rawson, J. M.; Alberola, A.; Whalley, A. *J. Mater. Chem.* **2006**, *16*, 2560–2565. (s) Benin, V.; Kaszynski, P. *J. Org. Chem.* **2000**, *65*, 8086–8088.

(2) (a) Preuss, K. E. *Dalton Trans.* **2007**, 2357–2369. (b) Hearns, N. G. R.; Preuss, K. E.; Richardson, J. F.; Bin-Salamon, S. *J. Am. Chem. Soc.* **2004**, *126*, 9942–9943. (c) Awaga, K.; Tanaka, T.; Shirai, T.; Fujimori, M.; Suzuki, Y.; Yoshikawa, H.; Fujita, W. *Bull. Chem. Soc. Jpn.* **2006**, *79*, 25–34. (d) Jennings, M.; Preuss, K. E.; Wu, J. *Chem. Commun.* **2006**, 341–343. (e) Britten, J.; Hearns, N. G. R.; Preuss, K. E.; Richardson, J. F.; Bin-Salamon, S. *Inorg. Chem.* **2007**, *46*, 3934–3945. (f) Hearns, N. G. R.; Clérac, R.; Jennings, M.; Preuss, K. E. *Dalton Trans.* **2009**, 3193–3203. (g) Hearns, N. G. R.; Fatila, E. M.; Clérac, R.; Jennings, M.; Preuss, K. E. *Inorg. Chem.* **2008**, *47*, 10330–10431.

(3) (a) Boeré, R. T.; Roemmele, T. L. *Coord. Chem. Rev.* **2000**, *210*, 369–445. (b) Boeré, R. T.; Moock, K. H. *J. Am. Chem. Soc.* **1995**, *117*, 4755–4760. (c) Boeré, R. T.; Moock, K. H.; Parvez, M. *Z. Anorg. Allg. Chem.* **1994**, *620*, 1589–1598.

(4) Ang, C. Y.; Boeré, R. T.; Goh, L. Y.; Koh, L. L.; Kuan, S. L.; Tan, G. K.; Yu, X. *Chem. Commun.* **2006**, 4735–4737.

(5) (a) Geevers, J.; Hackmann, T.; Trompen, W. P. *J. Chem. Soc. C* **1970**, 875–878. (b) Kornuta, P. P.; Derii, L. I.; Romanenko, E. A. *Chem. Heterocycl. Compd.* **1978**, *273*, 226. (c) Kornuta, P. P.; Derii, L. I.; Markovskii, L. N. *Zh. Org. Khim.* **1980**, *16*, 1308–1313. (d) Markovskii, L. N.; Kornuta, P. P.; Katchkovskaya, L. S.; Polumbrik, P. M. *Sulfur Lett.* **1983**, *1*, 143–145. (e) Hayes, P. J.; Oakley, R. T.; Cordes, A. W.; Pennington, W. T. *J. Am. Chem. Soc.* **1985**, *107*, 1346–1351. (f) Cordes, A. W.; Hayes, P. J.; Josephy, P. D.; Koenig, H.; Oakley, R. T.; Pennington, W. T. *J. Chem. Soc., Chem. Commun.* **1984**, 1021–1022. (g) Cordes, A. W.; Craig, S. L.; Condren, M. S.; Oakley, R. T.; Reed, R. W. *Acta Crystallogr.* **1986**, *C42*, 922–923. (h) Ramakrishna, T. V. V.; Elia, A. J.; Vij, A. *Inorg. Chem.* **1999**, *38*, 3022–3026. (i) Boeré, R. T.; Cordes, A. W.; Hayes, P. J.; Oakley, R. T.; Reed, R. W.; Pennington, W. T. *Inorg. Chem.* **1986**, *25*, 2445–2450. (j) Knapp, C.; Watson, P. G.; Lork, E.; Friese, D. H.; Mews, R.; Decken, A. *Inorg. Chem.* **2008**, *47*, 10618–10625. (k) Chen, S.-J.; Behrens, U.; Fischer, E.; Mews, R.; Pauer, F.; Sheldrick, G. M.; Stalke, D.; Stohrer, W.-D. *Chem. Ber.* **1993**, *126*, 2601–2607. (l) Cordes, A. W.; Oakley, R. T. *Acta Crystallogr.* **1987**, *C43*, 1645–1646. (m) Farrar, J. M.; Patel, M. K.; Kaszynski, P.; Young, V. G., Jr. *J. Org. Chem.* **2000**, *65*, 931–940. (n) Kaszynski, P. *J. Phys. Chem. A* **2001**, *105*, 7615–7625. (o) Kaszynski, P. *J. Phys. Chem. A* **2001**, *105*, 7626–7633.

(6) Oakley, R. T.; Reed, R. W.; Cordes, A. W.; Craig, S. L.; Graham, J. B. *J. Am. Chem. Soc.* **1987**, *109*, 7745–7749.

(7) Boeré, R. T.; Oakley, R. T.; Reed, R. W. *J. Organomet. Chem.* **1987**, *331*, 161–167.

(8) (a) Peak, D. A. *J. Chem. Soc.* **1952**, 215–226.(b) Oto, K.; Ichikawa, E. Patent Japan JP 48003811, 1973; *Chem. Abstr.* **1973**, *79*, 18443. (c) Liebscher, J.; Knoll, A.; Berger, A.; Krenzke, A. Patent East Ger. DD 219,479, 1985; *Chem. Abstr.* **1985**, *103*, 195834. (d) Brown, H. C.; Schuman, P. D. *J. Org. Chem.* **1963**, *28*, 1122–1127. (e) Schaeffer, F. C.; Hechenbleikner, I.; Peters, G. A.; Wystrach, V. P. *J. Am. Chem. Soc.* **1958**, *81*, 1466–1470.

(9) Peters, G. A.; Schaeffer, F. C. Patent: Ger 1,175,684; *Chem. Abstr.* **1964**, *61*, 14694c.

(10) Privett, A. J.; Craig, S. L.; Jeter, D. Y.; Cordes, A. W.; Oakley, R. T.; Reed, R. W. *Acta Crystallogr.* **1987**, *C43*, 2023–2025.

(11) (a) Kopylovich, M. N.; Pombeiro, A. J. L.; Fischer, A.; Kloo, L.; Kukushkin, V. Y. *Inorg. Chem.* **2003**, *42*, 7239–7248. (b) Gushchin, P. V.; Tyan, M. R.; Bokach, N. A.; Revenco, M. D.; Haukka, M.; Wang, M.-J.; Lai, C.-H.; Chou, P.-T.; Kukushkin, V. Y. *Inorg. Chem.* **2008**, *47*, 11487–11500. (c) Norrestam, R. *Acta Crystallogr.* **1984**, *C40*, 955–957. (d) Robinson, V.; Taylor, G. E.; Woodward, P.; Bruce, M. I.; Wallis, R. C. *J. Chem. Soc., Dalton Trans.* **1981**, 1169–1173. (e) Barker, J.; Kilner, M.; Mahmoud, M. M.; Wallwork, S. C. *J. Chem. Soc., Dalton Trans.* **1989**, 837–841. (f) Hursthouse, M. B.; Mazid, M. M.; Robinson, S. D.; Sahajpal, A. *J. Chem. Soc., Dalton Trans.* **1994**, 3615–3620. (i) Aris, D. R.; Barker, J.; Phillips, P. R.; Alcock, N. W.; Wallbridge, M. G. H. *J. Chem. Soc., Dalton Trans.* **1997**, 909–910.

(12) Pinkerton, A. A.; Schwarzenbach, D. *J. Chem. Soc., Dalton Trans.* **1978**, 989–996.

(13) Greenwood, N. N.; Earnshaw, A. *Chemistry of the Elements*, 2nd ed.; Reed Educational and Professional Publishing Ltd.: Oxford, U. K., 1997; p 60.

(14) (a) Boeré, R. T.; Moock, K. H.; Derrick, S.; Hoogerdijk, W.; Preuss, K.; Yip, J. *Can. J. Chem.* **1993**, *71*, 473–486. (b) Boeré, R. T.; Fait, J.; Larsen, K.; Yip, J. *Inorg. Chem.* **1992**, *31*, 1417–1423.

(15) Cordes, A. W.; Oakley, R. T. *Acta Crystallogr., Sect. C* **1987**, *C43*, 1645–1646.

(16) Boeré, R. T. Unpublished data.

(17) *CRC Handbook of Chemistry and Physics*, 70th ed.; Weast, R. C., Ed.; CRC Press: Boca Raton, FL, 1989; p F−188.

(18) Frisch, M. J.; Trucks, G. W.; Schlegel, H. B.; Scuseria, G. E.; Robb, M. A.; Cheeseman, J. R.; Zakrzewski, V. G.; Montgomery, J. A., Jr.; Stratmann, R. E.; Burant, J. C.; Dapprich, S.; Millam, J. M.; Daniels, A. D.; Kudin, K. N.; Strain, M. C.; Farkas, O.; Tomasi, J.; Barone, V.; Cossi, M.; Cammi, R.; Mennucci, B.; Pomelli, C.; Adamo, C.; Clifford, S.; Ochterski, J.; Petersson, G. A.; Ayala, P. Y.; Cui, Q.; Morokuma, K.; Malick, D. K.; Rabuck, A. D.; Raghavachari, K.; Foresman, J. B.; Cioslowski, J.; Ortiz, J. V.; Baboul, A. G.; Stefanov, B. B.; Liu, G.; Liashenko, A.; Piskorz, P.; Komaromi, I.; Gomperts, R.; Martin, R. L.; Fox, D. J.; Keith, T.; Al-Laham, M. A.; Peng, C. Y.; Nanayakkara, A.; Gonzalez, C.; Challacombe, M.; Gill, P. M. W.; Johnson, B.; Chen, W.; Wong, M. W.; Andres, J. L.; Gonzalez, C.; Head-Gordon, M.; Replogle, E. S.; Pople, J. A. *Gaussian 98*, Revision A.7; Gaussian Inc.: Pittsburgh, PA, 1998.

(19) Duling, D. R. *J. Magn. Reson., Ser. B* **1994**, *104*, 105–110.

(20) (a) Boeré, R. T.; Oakley, R. T.; Reed, R. W.; Westwood, N. P. C. *J. Am. Chem. Soc.* **1989**, *111*, 1180–1185. (b) Boeré, R. T.; Roemmele, T. L. *Phosphorus, Sulfur, Silicon* **2004**, *179*, 875–882.

(21) Moock, K. H.; Rock, M. H. *J. Chem. Soc., Dalton Trans.* **1993**, 2459–2463.

(22) (a) Lau, H. F.; Ang, P. C. Y.; Ng, V. W. L.; Kuan, S. L.; Goh, L. Y.; Borisov, A. S.; Hazendonk, P.; Roemmele, T. L.; Boeré, R. T.; Webster, R. D. *Inorg. Chem.* **2008**, *47*, 632–644. (b) Beekman, R. A.; Boeré, R. T.; Moock, K. H.; Parvez, M. *Can. J. Chem.* **1998**, *76*, 85–93.

(23) Oakley, R. T. *Prog. Inorg. Chem.* **1988**, *36*, 299–391.

(24) (a) Rudolph, M. J. *Electroanal. Chem.* **2003**, *543*, 23. (b) Rudolph, M. J. *Electroanal. Chem.* **2004**, *571*, 289. (c) Rudolph, M. J. *Electroanal. Chem.* **2003**, *558*, 171. (d) Rudolph, M. J. *Comput. Chem.* **2005**, *26*, 619. (e) Rudolph, M. J. *Comput. Chem.* **2005**, *26*, 1193.

(25) (a) Evans, D. H. *Chem. Rev.* **1990**, *90*, 739–751. (b) Evans, D. H. *Chem. Rev.* **2008**, *108*, 2113–2144.

(26) Izutsu, K. *Electrochemistry in Nonaqueous Solutions*, 2nd ed.; Wiley-VCH: Weinheim, Germany, 2009; p 100ff.

(27) Boeré, R. T.; Bond, A. M.; Chivers, T.; Feldberg, S. W.; Roemmele, T. L. *Inorg. Chem.* **2007**, *46*, 5569–5607.

(28) Sheldrick, G. M. *Acta Crystallogr., Sect. A* **2008**, *A64*, 112–122.